الجمهورية الجـزائـريـة الديمقراطـيـة الشـعـبيـــة

وزارة التعليم العـــالي والبـحـث العلمـي

PEOPLE'S DEMOCRATIC REPUBLIC OF ALGERIA MINISTERY OF HIGH EDUCATION AND SCIENTIFIC RESEARCH

جـامعة سـعد دحلـب البلـيـــدة 1

UNIVERSITY OF SAAD DAHLEB BLIDA 1

كلية العلوم – دائرة الفيزياء

Faculty of science - Department of Physics

MASTER DIPLOMA IN PHYSICS

Option: Nanophysics

THEME

THICKNESS EFFECT ON POST-ANNEALED VANADIUM OXIDE THIN FILMS DEPOSITED BY THERMAL EVAPORATION TECHNIQUE

By :

-FERHI SANAA

-BOUCHELAREM MANEL

Jury Members :

Dr. Salah Eddine Aoudj	MCA,	U.Blida1	President
Dr. Abdelkader Hassein-Bey	MCB,	U.Blida1	Examiner
Dr. Slimane Lafane	MRB,	CDTA	Advisor
Asma.L.S Hassein-Bey	U.Blida1/CDTA		Co-Advisor

2019 / 2020

Abstract

In this Study, vanadium oxide thin films are prepared by thermal evaporation technique deposited on glass and silicon substrates, the V_2O_5 powder mass was varied from 15mg , 25mg, 50mg to 70mg to realise a different layer's thicknes. The films are electrically studied by bolometer to determine TCR (Temperature coefficient of resistance) for different thickness before annealing, then the films were annealed under temperature of 400°C for 5 min to obtain another electrical results and to obtain others values of TCR with annealing assess. Finally the annealed thin films was structurally studied to guess the different oxide vanadium phases for each thickness.

Résumé

Dans cette étude, des couches minces d'oxyde de vanadium sont préparés par évaporation thermique et déposée sur un substrat de verre et de silicium, la masse de poudre de V_2O_5 a été variée de 15 mg, 25 mg, 50 mg à 70 mg pour réaliser une épaisseur de couche différente. Les couches sont étudiées électriquement par le bolomètre pour déterminer le TCR (coefficient de température de résistance) pour différentes épaisseurs avant le recuit, puis les couches ont été recuits à une température de 400 ° C pendant 5 min pour obtenir un autre résultat électrique et pour obtenir d'autres valeurs de TCR avec un procédé de recuit. Enfin, les couches minces recuites ont été étudiées structurellement pour examiner les différentes phases d'oxyde de vanadium pour chaque épaisseur.

ملخص

في هذه الدراسة يتم تحضير طبقات رقيقة من اكسيد الفاناديوم بالتبخير الحراري موضوعة على طبقة من زجاج و سيليسيوم مع التغيير من كتلة المسحوق في كل مرة (15 ميلي غرام ، 25 ميلي غرام، 50 ميلي غرام الى غاية 70 ميلي غرام) و هذا لهدف تحقيق عدة سمكات لعدة طبقات ،كما قمنا بدراسة هذه الطبقات كهربائيا لتحديد المعامل الحراري للمقاومة قبل التسخين .

بعد ذلك قمنا بتسخين الطبقات الرقيقة ب 400 درجة مئوية لمدة 5 دقائق و هذا من اجل الحصول على مختلف نتائج كهربائية ومعامل حراري مختلف للمقاومة .

أخيرًا ، تمت دراسة الطبقات الرقيقة الملدنة هيكليًا لتخمين المراحل المختلفة لأكسيد الفاناديوم لكل منها سماكة خاصة.

Acknowledgments

At the end of this work, we would like to thank Allah the Almighty for us to have given the courage, the will and the patience to complete this work.

To our parents,

We thank our dear parents, who have always been there for us, “You sacrificed everything for your children sparing neither health nor effort. You had given a magnificent model of hard work and perseverance. We are indebted to a education of which we are proud ”.

They were able to give us every chance to succeed. That they find, in the achievement of this work, the culmination of their efforts as well as the expression of our most affectionate gratitude. We thank our sisters who have been with us all throughout this year. who shared a lot with us.

The work presented in this thesis took place at the Center de development of advanced technologies in ALGIERS (CDTA).

First , we would like to thank **Dr. Slimane LAFANE,** It is a great honor for us to see you sit on our jury.You have done us the great honor of agreeing to lead us in this work with kindness and rigor. Your dedication to a job well done is the object of my consideration.Your professional background, your undeniable competence, your charisma and your human qualities make you a great teacher and we inspire great admiration and respect.Your kindness, your dynamism, your dedication to work and your competence aroused our admiration.We take this opportunity to express our gratitude to you for the time you spent doing this job.We pray, dear Master, to accept our deep gratitude and our high consideration.

Secondly, we would be more than glad to thank our Co-advisor **Asmaa Leila Sabeha HASSEIN-Bey ,** We have had the privilege of working with you and appreciating your qualities and values.Your seriousness, your competence and performance, your sense of duty have left a huge mark on us.Please find here the expression of our respectful consideration and our deep admiration for all your scientific and human qualities. May generations and generations have the chance to benefit of your knowledge which is matched only by your wisdom and kindness. Allow us, dear Co-Advisor to express to you our deep respect and our sincere gratitude.

We acknowledge warmly ionized medium & laser division especially the Laser matter interaction group also Microelectronics & Nanotechnology Division of the **CDTA** for the easiness and the good progress of work. The authors would like to thank **Mr.Nait Bouda Lamine**, We thank you for your support, sound advice and your precious help, thank you very much. **Mr.Lekoui Fouaz,** thank you for your kindness and your precious help**. Mr.Malek Smail,** thank you for your precious help and advices.

We also thank physics department of BIRINE nuclear research center **CRNB. Mr.Sari Ali,** We take this opportunity to express our deep gratitude to you while showing you our respect.

To our Master, Option manager “Nanophysics”
Dr.Abdelkader Hassein-Bey

It is a great honor for us to see you sit on our jury. We have had the great pleasure of working under your guidance, and we found with you the advisor and the guide who received us in all circumstances with sympathy, smile and kindness. You are a man of science and an attentive teacher, your incontestable professional competence as well as your human qualities you worth everyone's admiration and respect. You are and you will be for us the example of rigor and righteousness in the practice of the profession. We have fond memories of the quality of teaching that you have lavished on us.

We would address our acknowledgements to the members of the jury, starting with the president of the jury “Dr.Salah Eddine Aoudj”, the examiner “Dr. Abdelkader Hassein-Bey”, and the advisors “Dr. S. Lafane” and “ A.L.S Hassein-Bey”, for giving us the honor to examine this work, and for the time and efforts that they have taken to read and correctthis manuscript. We will certainly not forget all the teachers that taught us through all these academic years.

At last not least, it is more than a pleasure to address our acknowledgement to our family members, friends and every person that gave us material and emotional support, just to push us to study and reach this level.

Dedicate

TO MY VERY DEAR MOTHER,

To the sweetest and most wonderful of all moms.
To a person who gave me everything without counting.
Inexhaustible source of tenderness, patience and sacrifice.

As many phrases as expressive as they are, cannot show the degree of love and affection I feel for you. You showered me with your tenderness and affection all along of my journey. You have never stopped supporting and encouraging me during all the years of my studies. Your prayers have been a great support for me throughout my studies.

Whatever I may say and write, I could not express my great affection and deep appreciation. Hope I never disappoint you.

I dedicate this work to you which, thanks to you, was able to see the light of day. I dedicate this memory to you which make your dearest dream come true, which is only the fruit of your advice and encouragement.

You have not stopped supporting and encouraging me, your love, your generosity exemplary and your constant presence made me who I am today.

I hope you will find in this modest work a testament to my gratitude, my deep affection and deep respect.

May Almighty Allah protect you, give you long life, health and happiness so that I can give you back a minimum of what I owe you.

I love you mom...

Ferhi sanaa

TO MY VERY DEAR FATHER,

To the one who helped me discover "knowledge" the inexhaustible treasure.
Of all the fathers, you are the best, you knew how to surround me with attention, instill in me values nobles of life, teach me the meaning of hard work, honesty and responsibility.

You have been and you will always be an example to follow for your qualities, your perseverance and your perfectionism.

Words can never express the depth of my respect, my consideration, my gratitude and my eternal love.

May this modest work be the fulfillment of your wish, the fruit of your countless sacrifices, though I never forgive you enough.

May Allah preserve you from the misfortunes of life so that you may remain the illuminating torch my way...

I love you dad ...

Ferhi sanaa

TO MY VERY DEAR SISTER Hanaa,

A sister like you can't find anywhere else, may Allah protect you, to keep and strengthen our fraternity.

You were and by my side during all the stages of this work.

I wish you success in your life, with all the happiness you need to fill you up.

I dedicate this work as a testament to my love and attachment.

I wish you all the happiness in the world.

Ferhi sanaa

List of contents

CHAPTER I : Vanadium Oxides as Microbolometer Sensing Material

I.1.Introduction ……...1
I.2.Vanadium……..….1
I.2.1. Physical Properties……..2
I.2.2. Chemical Properties……2
I.3.Vanadium oxides…….…….……..3
I.3.1 Vanadium monoxide……3
I.3.2 Vanadium Trioxide…….……3
I.3.3 Vanadium Pentoxide…….…….……..4
I.3.4 Vanadium Dioxide…….……...…4
a.General Characteristics of VO_2.……..……..……..4
b.Crystallographic Structure……..…..……4
c.Band Structure……..……..….……...5
d.Electrical and Optical Properties……..……6
I.4.VOx for infrared Applications……..……8
I.4.1 The difference between uncooled IR detectors and Photonic detectors……..9
I.4.2 Definition of a Microbolometer……9
I.4.3 The role of a Microbolometer……10
I.4.4 The characteristics of a Microbolometer……10
I.4.5 The Materials used……10
I.4.6. Micro-Fabrication Process……11
I.5.State of The Art……12
I.6.Conclusion……...……15

CHAPTER II : Thin Films Generalities

II.1.Introduction……..……..16
II.2.Definition of thin Layer …….……16
II.3.Thin films deposition precedure ……17
II.3.1.Physical vapour deposition procedure (PVD)……..17

II.3.2.Atomic Layer Deposition ……18
II.4.Characterization technique for diposited films……..…..18
II.4.1.Stuctural and surface analyse……18
a.X-ray diffraction……...18
b.Scanning Electron Microscope……21
II.4.2.Morphology and thickness analysis……..23
a.Profilometer Device……..23
II.4.3.Electrical properties analysis……24
a.Four-pointed technique……24
II.5. Experimental Procedure……25
II.5.1 Nature of Substrate……25
II.5.2 Preparation of Substrate……..……..25
II.5.3 The Deposition Procedure……..……..……26
II.5.4 Annealing Procedure…….……27
II.6. Conclusion……29

CHAPTER III :RESULTS AND DISCUSSIONS

III.1.Introduction……..……30
III.2.Surface Morphology……..30
a) Thickness Measurements ……..30
b) Surface Morphology ……..……31
III.3.structural analysis……..……33
III.4.Electrical Measurement……...……..34
III.4.1. Resistance Measurement……...……34
III.4.2. V-I Characteristics……...……..36
III.4.3. Temperature dependence of Resistivity…….……39
a)Electrical properties stabilisation upon multiple thermal cycling…….…….39
b)Effect of the Thickness on the electrical Resistivity……..…41
III.4.4. Temperature coefficient of resistance (TCR) Measurement……...42
a) Thickness dependence of the temperature coefficient of resistance (TCR)……...…… 42
b) Bias current dependence of the temperature coefficient of resistance (TCR)……...……43
III.5.Conclusion……...……46
General conclusion 47
Reference Bibliographic.....48

List of figures

Chapter I

Figure1.1: A Sample of Vanadium……..……..……2

Figure1.2: Low temperature monoclinic VO_2 (M1) structure and high temperature rutile (R) structure……...……...5

Figure1.3 : VO_2 band structure representing the insulating-metal transition…….……..…….6

Figure1.4: Optical and Electrical properties of VO_2 thin film ……...…….....…7

Figure1.5: Electrical Resistivityversus temperature for several oxides of vanadium, across the Semiconductor-Metallic Transition……..…..7

Figure1.6: Temperature dependent transmission change is seen for various wavelengths….....8

Figure1.7: a)SEM image of the processed bolometer pixel. Pixel size: 65 µmX60µm,
b)A microbolometer pixel structure……9

Figure 1.8: The structure of the designed microbolometer……..11

Figure 1.9: Schematic diagram showing the processes of microbolometer suspended structure…….……12

Figure1.10: The resistivity at 300°K vsTCR plot of pulsed DC data including regions denoting microstructural character…….…….……..14

Chapter II

Figure2.1: schematic of thin film deposited on a glass substrate…….……..16

Figure2.2 :A schematic representation of Bragg's law……..……... ..20

Figure2.3: Configuration of grazing incidence X-ray diffraction setup……...21

Figure2.4: Detailed schematic of the working principle of a scanning electron microscope and (b) a photographic image of the SEM used for analysis in this study……22

Figure2.5 : Surface SEM micrographs of the as deposited VO_X film (a) with a nanocrystalline morphology. (b) & (c) show the surface micrographs of V_2O_5 and VO_2 formed after oxidation and reduction treatments respectively…….……..23

Figure2.6: Four-point measurement of resistance between voltage sense connections 2 and 3. Current is supplied via force connections 1 and 4……....25
Figure2.7 : The deposition method of VOx thin layers in a vacuum chamber(CDTA)……..27
Figure2.8 : Photograph of the annealing device (CDTA)……..……..28
Figure2.9: Annealing Process treatment…….....28

Chapter III

Figure3.1: Films thickness versus the evaporated mass. The dashed line is a guide to the eye....31
Figure3.2: SEM image of evaporated and annealed VOx thin layer (70 mg)……..…...32
Figure3.3: SEM image of evaporated and annealed VOx thin layer (50mg)……..…32
Figure3.4: SEM Image of evaporated and annealed VOx thin layer (25mg)……..…32
Figure 3.5: SEM Image of evaporated and annealed VOx thin layer (15mg)…….....33
Figure 3.6: Grazing XRD patterns of as-deposited and annealed VOx thin films……..…34
Figure 3.7: (V-I) Characteristics of as-deposited VOx thin films at different thickness (a) 56nm, (b) 95 nm , (c) 150nm, (d) 191nm……...……..36
Figure 3.8: (V-I) Characteristics of annealed VOx thin films with different thickness (a) 95 nm, (b) 150 nm, (c) 191 nm……..37
Figure3.9: Bias Current threshold versus films thickness……...……38
Figure 3.10: Sheet Resistance of as-deposited VOx thin films upon first thermal cycling (**a)** 56nm**, (b)** 95nm, **(c)** 150nm, **(d)** 191nm. The bias current is 0,5 µA……..39
Figure3.11: Sheet Resistance of as deposited VOx thin films upon multiple thermal cycling (a) 150 nm under 2nd cycle, (b) 190 nm under 2nd cycle and (c) 190 nm under 3rd cycle. The bias current is 0,5 µA……40
Figure 3.12: Typical sheet Resistance behaviour of annealed VOx thin films upon multiple thermal cycling. The thickness of the film is 190 nm……..…41
Figure 3.13. Electrical resistivity at room temperature (300°K) of as-deposited and annealed VOx thin films……..41

Figure 3.14. Thickness dependence of the temperature coefficient of resistance (TCR) at room temperature……42

Figure 3.15: Bias current dependent voltage-temperature characteristics of as-deposited 191 nm thick films……43

Figure 3.16: Hysteresis loop of As-deposited 191 nm thick films resistance versus temperature at bias current of 25 µA. ……..…… 44

Figure 3.17: Bias current dependent TCR at room temperature of as-deposited 190 nm thick films……..45

Figure 3.18: TCR versus resistivity of as-deposited and annealed VOx thin film……..45

List of tables

Chapter II

Table II.1 The main deposition parameters of VOx films……26

Chapter III

Table.III.1 VOx thin layers Thickness deposited on glass and Silicon substrates…….30

Table.III.2 Resistance Measurement of 191 nm films thickness……...35

Table.III.3 Resistance Measurement of 150 nm films thickness……...35

Table.III.4 Resistance Measurement of 95 nm films thickness…….35

Table.III.5 Resistance Measurement of 56 nm films thickness…….……35

List of equations

Chapter I

A Metal oxidized by a current of Hydrochloric acid bubbling in contact……..…….2

B Vanadium react with nitric acid to produce nitrate-dioxide vanadium, nitrogen dioxide and water……3

C Vanadium reacts with fluorine, F_2, when heated, forming form vanadium(V) fluoride…..3

D Vanadium metal reacts with excess oxygen, O_2, upon heating to form vanadium(V) oxide, V_2O_5..... 3

1 Voltage Responsivity……12

2 Temperature Coefficient of Resistance……..13

List of abbreviations

Chapter I

SMT Semiconductor-Metallic Transition……08
TCR Temperature Coefficient of Resistance…….……..10
CMOS Complementary Metal Oxide Semiconductor…….10
MEMS Micro-Electro-Mechanical Systems…….……...11
PECVD Plasma Enhanced Chemical Vapour Deposition……11
RIE Reactive Ion Etching……...…11
DC Direct current……...……14
FCC Face-Centred Cubic…….14

Chapter II

PVD Physical Vapor Deposition……..17
ALD Atomic Layer Deposition……18
TEMAV Tetrakis Ethyl Methyl Amino Vanadium…….18
TDMAV Tetrakis Dimethyl Amino Vanadium……..18
TDEAV Tetrakis Diethyl Amino Vanadium……18
SEM Scanning Electron Microscope……21

General Introduction

In strongly correlated electron systems, observed electronic and structural behaviours result from the complex interplay between multiple, sometimes-competing degrees-of freedom. As a result, these materials exhibit a variety of unusual behaviours, such as high-temperature superconductivity, colossal magneto resistance, exotic magnetic, charge and orbital ordering, and insulator to- metal transitions. Oxides of vanadium are typical strongly-correlated materials that have been widely-studied by theoretical and experimental condensed-matter and materials community for more than half a century. Among all the oxides of Vanadium, Vanadium di oxide (VO_2) and Vanadium pentoxide (V_2O_5) are of particular interest and they enjoy a cult following in the research community and for good reasons. VO_2 and V_2O_5 have been the materials of choice to understand fundamental exciting physics and were implemented for the innovative industrially relevant applications.

Our work was based on the study of oxides vanadium thickness and its influence on electrical and structural properties, by varying the thickness and carry out an electrical measure of resistance and deduce resistivity and TCR (temperature coefficient of resistance),and make a structural study of different thickness obtained by taking into consideration the results of the last year as working conditions, such as annealing conditions (400°C_5min), since our work is the continuity of a work already done. finally, the reason of this work is how to obtain a thin and sensitive film of vanadium oxide to exploit it for several requirements.

Chapter 01 of the memory deals with the basic structures, properties and background of Vanadium oxides, we focused on the optical and electrical of VOx thin films properties followed by a brief review on the VOx for infrared applications.

Chapter 02 of the memory reviews the overview about thin films and theirs deposition techniques, and characterisation methods that are used in our work. In depth, details about the experimental aspects pertaining to this thesis are provided in this chapter, whereas results and discussion are detailed in **chapter 03**.

CHAPTER I
Vanadium Oxides as Microbolometer Sensing Material

I.1.Introduction

Vanadium is the thirty-second element in order of abundance in the earth's crust. It is widely distributed in nature but is widely dispersed. Detected in meteorites and in many stars, including the Sun, it is present in small quantities in seawater and in living beings, both in the plant and animal kingdoms, which shows its biological importance. Vanadium oxide is composited of several oxides as V_2O_5, V_2O_3, V_6O_{13}, and VO_2[1].

It represents many proprieties such as electrical, chemical, optical properties what they make it useful for several technological applications for example: smart window, gas-sensorsect….

I.2.Vanadium

Vanadium is chemical element of symbol V, atomic number 23 and electronic configuration [Ar] $3d^3\,4s^2$the 23rd element in Mendeleyev's periodic table, was first discovered in 1801 within a lead vanadate ore by Andrés Manuel del Río a Spanish mineralogist in Mexico city, but it was mistakenly identified as chromium, during his experiments. He discovered that this colour came from traces of chromium, and then renamed the element panchromium. He later renamed it Erythronium again, as most of the salts turned red when heated. The French chemist Hippolyte-Victor Collet-Descotils declared then that the new element of del Rio was only impure chromium .The element was rediscovered in 1831 within converter slags from certain iron ore by Swedish chemist Nils Gabriel Sefström, who named it vanadium after the Scandinavian goddess of beauty and fertility[2-3].

Figure1.1: A Sample of Vanadium[2].

I.2.1. Physical Properties

A silvery white metal, vanadium is also hard and metallic-looking solid. Ductile means capable of being drawn into thin wires.It is pure of excellent mechanical characteristic and can work itself cold and hot,its melting point is about 1,900°C (3,500°F) and its boiling point is about 3,000°C (5,400°F). Its density is 6.11 grams per cubic centimeter.

Vanadium is special in that it acts like a metal in some cases, and as a non-metal in other cases,is available in many forms including foil, granules, powders and stems[4-5].

I.2.2. Chemical Properties

Vanadium is moderately reactive. It does not react with **oxygen** in the air at room temperatures, nor does it dissolve in water. It does not react with some acids. But it does become more reactive with hot acids, such as nitric acids and Hydrochloric Acid.[4-6]

- The Metal can be oxidized by a current of Hydrochloric acid bubbling in contact with it:

$$V(s) + 2HCl^{-}(l) \longrightarrow V^{2+}(aq) + H_2(g) + 2Cl^{-}(aq) \qquad (A)$$

- Vanadium react with nitric acid to produce nitrate-dioxide vanadium, nitrogen dioxide and water:

$$V(s)+6HNO_3(l) \longrightarrow VO_2NO_3(l)+5NO_2(g)+3H_2O(l) \quad (B)$$

- Vanadium reacts with fluorine, F_2, when heated, forming form vanadium(V) fluoride:

$$2V(s) + 5F_2(g) \longrightarrow 2VF_5(l) \quad (C)$$

- Vanadium metal reacts with excess oxygen, O_2, upon heating to form vanadium(V) oxide, V_2O_5:

$$4V(s) + 5O_2(g) \longrightarrow 2V_2O_5(s) \quad (D)$$

I.3.Vanadium oxides

In the environment, vanadium offers a complex chemistry and a complex crystal system and consist of various composition of vanadium and oxygen, each identifiable by its lattice structure and spacing group [7]. As a consequence of its multivalent character, it has a number of possible oxidation states (V^{+2}, V^{+3}, V^{+4}, V^{+5}), which form an extensive list of binary V−O systems. Some of them are grouped in theso-called "Magneli phases," with stoichiometric formula **V_nO_{2n-1}**, and others in the Wadsley phases, with stoichiometric formula **V_nO_{2n+1}**. The most commonly used phases, found in various applications due to their particular properties, are the VO, VO_2, V_2O_3, and V_2O_5 oxide phases.[8]

I.3.1. Vanadium monoxide

VO is one of the many vanadium oxide phases with crystalline cubic structure and good electrical conductivity.

I.3.2. Vanadium Trioxide

V_2O_3 phase, like VO_2 compound, presents an abrupt conductivity change at a temperature around 160°K, evidenced of a metal-insulator transition. In addition, it presents a

thermochromic behaviour in the infrared band [9].

I.3.3. Vanadium Pentoxide

V_2O_5 is the most stable of all vanadium oxide phases, and the preferred one to be used as thermoresistive material in microbolometer arrays for thermal imaging due to its high TCR value. Vanadium pentoxide is a semiconductor with a bandgap of 2.1–2.4 eV, which presents the following polymorphs: α- V_2O_5 (orthorhombic), β- V_2O_5 (monoclinic or tetragonal), and γ- V_2O_5 (orthorhombic), being the α-polymorph the most stable one [9].

I.3.4. Vanadium Dioxide

VO_2 is an amphoteric compound with the unique property of changing from a semiconductor monoclinic phase to a (semi)metal tetragonal rutile phase at a temperature around 340°K and, therefore, its electrical resistivity together with the optical properties also change up to several orders of magnitude between these two states [10].

a. General Characteristics of VO_2 :

VO_2 is a transition-metal oxide which undergoes metal–semiconductor phase transition at about 68°C. It has potential application in optical and electrical switches, data storage, laser shield and uncooled infrared detector. In recent years, it has been intensively studied in both theory and experiments[11].

b. Crystallographic Structure:

Vanadium dioxide is found in different structures depending on temperature conditions.The two main structures of vanadium dioxide are:

- A monoclinic structure for the semiconductor phase at room temperature or below, often denoted "M1". **(Fig1.4.a)**
- A rutile tetragonal structure for the metallic phase at temperatures above 68°C / 340 °K often denoted "R".**(Fig1.4b)**

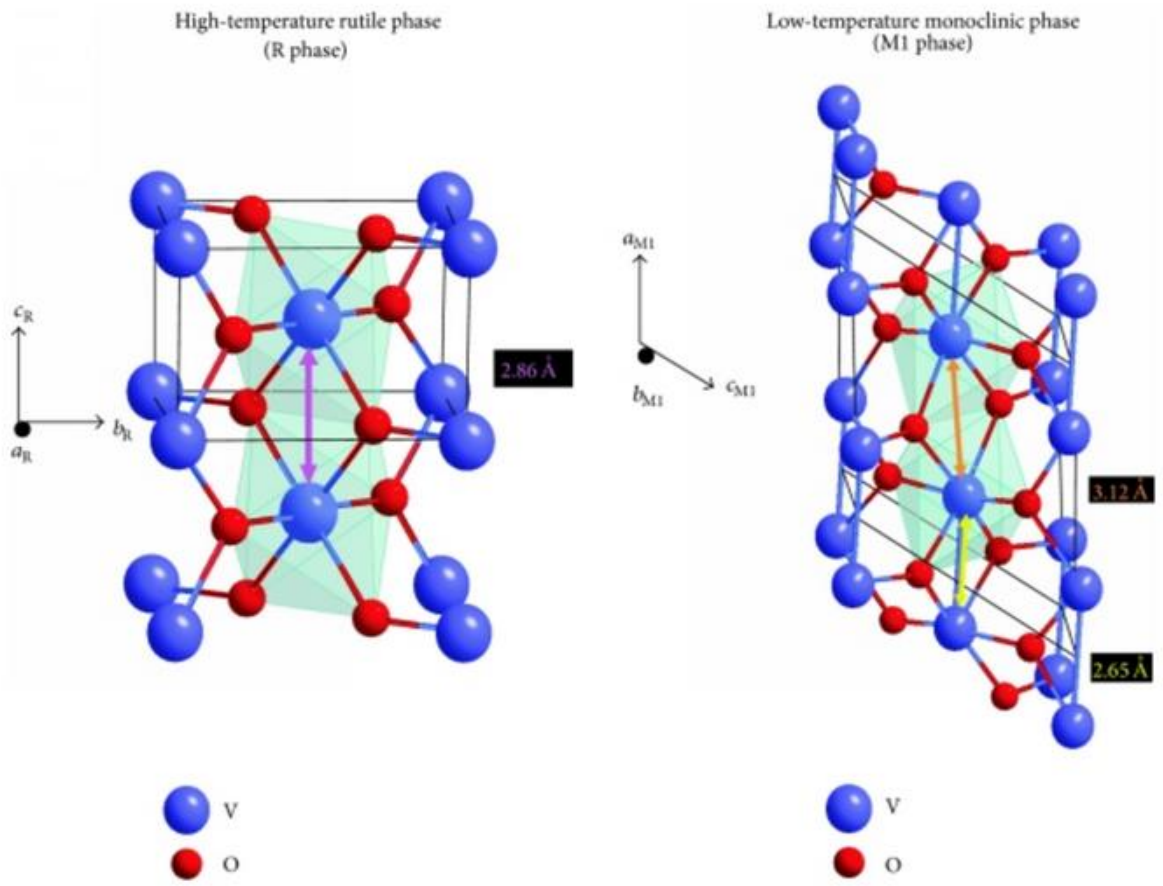

Figure 1.2: Low temperature monoclinic VO_2 (M1) structure and high temperature rutile (R) structure[12].

A different structural arrangement is observed on either side of the isolation metal transition in VO_2. Indeed, vanadium dioxide passes from a monoclinic structure (M1) at low temperature to a quadratic structure / Rutile (R) at high temperature. **Figure1.2** illustrates the VO_2 structures in both insulating and metallic states[13].

c. Band Structure:

During its transition from insulation to metal phase, the VO_2 band structure also changes. In the metallic state, the VO_2 structure consists of two bands; a 3d// binding band and an anti-binding band 3dπ*. By moving from the metal phase to the insulating phase during the TIM, the 3d// band is divided in two. We therefore find a filled binder strip with a lower energy called 3d// and another empty anti-binder strip with a higher energy called 3d//*. Finally, the binding strip 3dπ* is pushed to a higher energy[13]. As a result, a band gap and therefore a gap Eg of

[0.6-0.7] eV appears in the insulating phase [13]. In the monoclinic phase, metal-metal pairing within the vanadium chains parallel to the rutile c axis causes splitting of the dk band into filled bonding and empty antibonding states. In contrast, the 3dπ∗bands move to higher energies due to the antiferroelectric zigzag-type displacement of the vanadium atoms. As a result, a band gap opens between the bonding dk band and the other t2g bands[14].

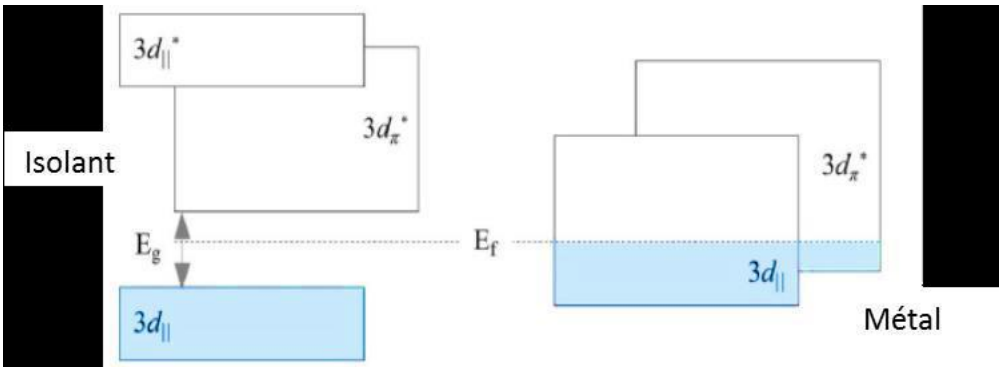

Figure 1.3: VO_2 band structure representing the insulating-metal transition [15].

d. Electrical and Optical Properties:

The vanadium dioxide phase transition occurs near 68°C. In this transition VO_2 shifts from a monoclinic to a tetragonal crystal structure, accompanied by large changes in electrical and optical behaviour. It is not uncommon to observe changes in the resistivity of more than 4 orders of magnitude as the temperature is cycled through the phase transition.With a bandgap energy of -0.6-0.7 eV, the semiconductor phase shows a high infrared transmittance.Optical and resistivity data for VO_2 thin films show hysteretic behavior, as shown in**Fig1.4**[16]. Insulator VO_2 has high transmittance whereas metallic VO_2 becomes opaque to near-IR radiation. Metal insolator transition behaviour of VO_2 is not only accompanied by significant change in infrared transmittance but also sharp change in resistivity. The transition takes place in approximately 80 fs, which is useful property for switching applications[17].

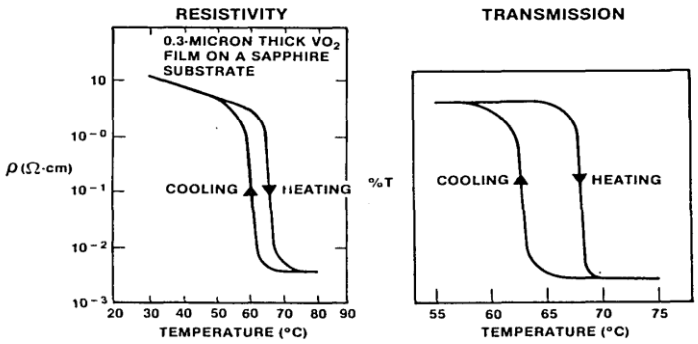

Figure1.4: Optical and Electrical properties of VO_2 thin film[16].

In single crystals, the resistivity change reaches a factor of 10^5 over a temperature range of 0.1 K . Hysteresis associated with this transition is of about 2 K. The conductivity jump and the narrowness of the hysteresis loop are very good indications of how close the stoichiometry is to VO_2. Small deviations destroy the sharpness of the transition and increase the hysteresis width[18].

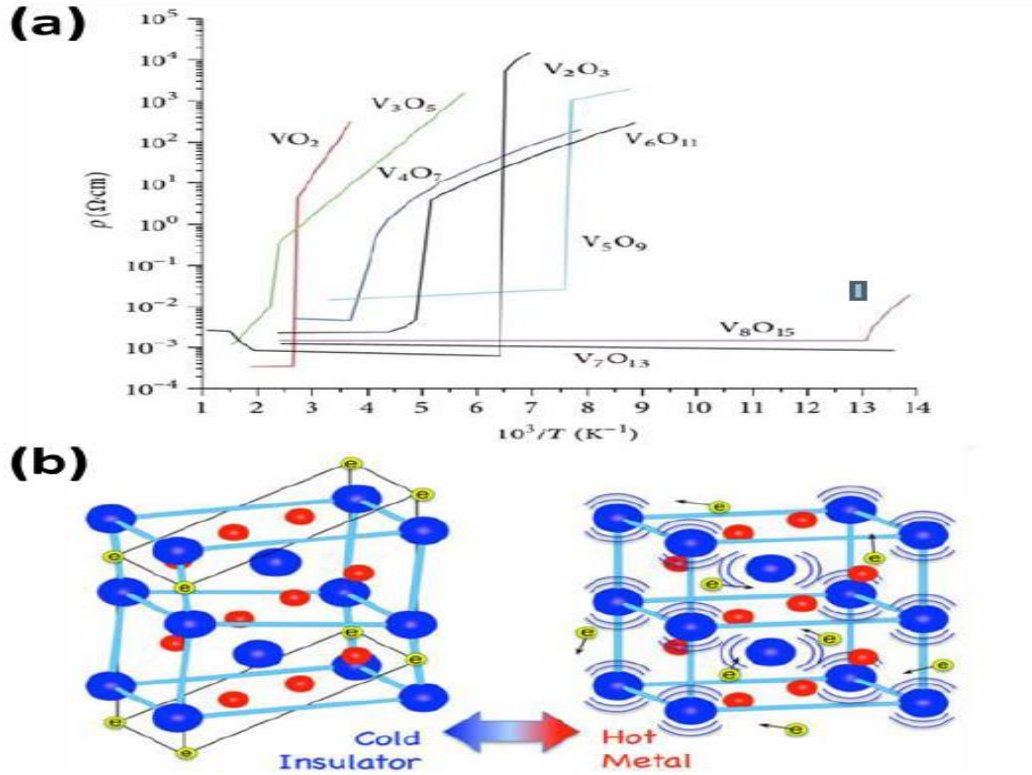

Figure1.5: Electrical Resistivityversus temperature for several oxides of vanadium, across the Semiconductor-Metallic Transition [19].

Figure1.5(a) shows the Electrical resistivity across the SMT in various vanadium oxide phases and **Figure1.5(b)**the Changes in the crystal structure and electronic properties of vanadium dioxide (VO_2) occur during its Semiconductor-Metal Transition (V blue; O red). Above 67°C (right), large-amplitude, nonlinear lattice vibrations (phonons) lead to a tetragonal crystal structure with mobile electrons (yellow) indicating that the VO_2 is a metal. At lower temperatures (left), the electrons are localized in the atomic bonds in the distorted monoclinic crystal structure indicating that the VO_2 is an insulator [19].

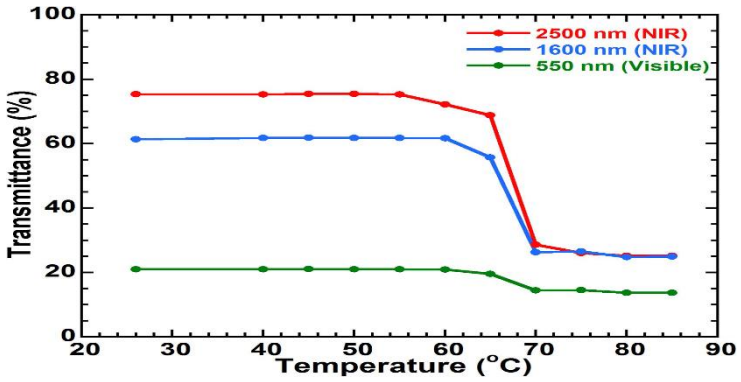

Figure1.6: Temperature dependent transmission change is seen for various wavelengths [17].

Fig1.6 indicates the temperature dependent transmittance of deposited 125 nm VO_2 thin films grown under 2.25% oxygen flow ratio at the wavelengths of 1600 and 2500 nm for near infrared and 550 nm for visible regions. In visible region, transmittance varies 7% with temperature, and it is about 21% at low temperatures. In addition, transmittance change at Metal-Insolator Transition region is around 36% for 1600 nm and 50% for 2500 nm wavelength. It is concluded that transmittance of insulator VO_2 phase is higher for 2500 nm than that of 1600 nm wavelength[17].

I.4.VOx for infrared Applications

Vanadium oxides are applicable in technology such as memory devices and temperature sensors [20], infrared-based night vision sensors are a unique technology because they can operate in the absence of visible light and offer significant advantages over other methods of night vision. Infrared detectors can be classified broadly into two categories: **uncooled IR detectors** and **photonic detectors**[21].

I.4.1. The difference between uncooled IR detectors and Photonic detectors

Photonic IR detectors: the absorption of a photon creates a pair of electron hole to be detected. The need for cooling because the quantity of electron-hole created is low compared to that already present and which due to thermal effects.

The photonic IR detectors have small band gaps at room temperature (~4 kT) and have excellent sensitivity. However, the photonic IR detectors exhibit large dark currents at and above room temperature such that during operation these currents will swamp the detecting signal without cryogenic cooling systems [22-23].

Uncooled IR detectors: IR radiation heats the sensitive layer and consequently changes its resistance. it operates at room temperature. slow response, consumes less energy**.**

The uncooled IR detector have many advantages over photonic detectors: they are portable, have a wide spectral response compared with semiconductor based photon detectors and have simple package form factors due to the absence of a cooling system. [22-23]

There are three most common thermal detectors; **thermoelectric detectors** (thermopiles), **pyroelectric detectors** and **resistive microbolometers**.

I.4.2. Definition of a Microbolometer:

A bolometer at temperature **T** is a thermal IR infrared sensor (detector) that uses a material with a temperature-dependent resistance ***R(*T)** to measure the heating effect of absorbed IR radiation.

a) **b)**

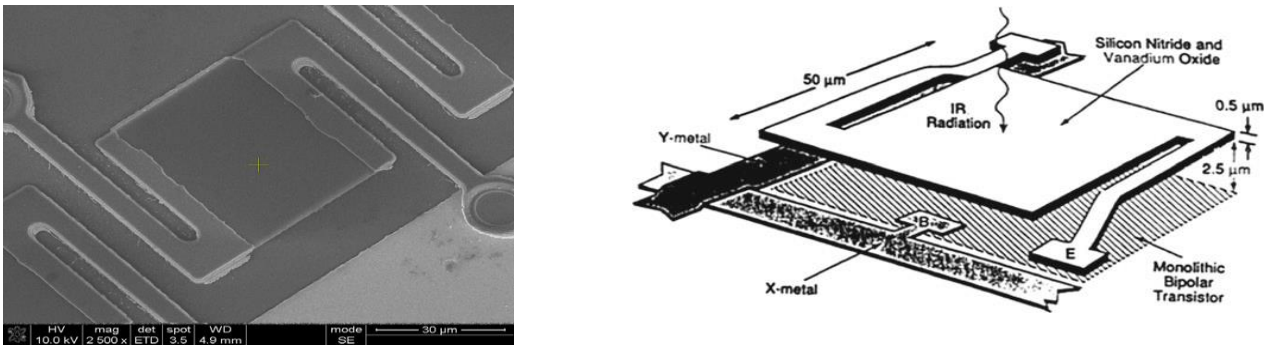

Figure1.7: **a)**SEM image of the processed bolometer pixel. Pixel size: 65 µmX60µm[23].
b)A microbolometer pixel structure[24].

I.4.3. The role of a Microbolometer

An uncooled bolometer measures variation in resistance in a thermally isolated semiconductor thin film pixel that has been exposed to IR light to detect temperature changes[22]. It can be used in infrared imaging applications such as thermal camera, night vision camera, surveillance, mine detection, early fire detection, medical imaging, and detection of gas leakage[25].

I.4.4. The characteristics of a Microbolometer

To achieve high temperature resolution capability, the required characteristics for a suitable uncooled bolometer material are [22]:

-a) high temperature coefficient of resistance (TCR)

-b) Moderate resistivity

-c) low 1/*f* noise

-d) Capable of absorbing the infrared radiation

I.4.5. The Materials used

The temperature resolution capability of an infrared sensor is inversely proportional to the absolute value of the TCR of the pixel material. A few materials that are under consideration as active detector elements for microbolometers are silicon, metal oxides, spinels and poly silicon-germanium[26].

- **The importance of choosing vanadium oxide:**

Of these materials, mixed valance vanadium oxide (VO*x*) thin films, have emerged as the leading commercial material for uncooled bolometer applications[27].

Vanadium oxide has been widely used in thermal devices due to its high temperature coefficient of resistance (TCR) value as well as its ability to operate at room temperature, and offers the best performance in terms of sensitivity and noise.

Lack of the need for cryogenic cooling results in lower cost of fabrication and bulkiness of the overall device[28].This material satisfies current complementary metal oxide semiconductor (CMOS) technology requirements with the thickness values between 50 and 100 nm[26].

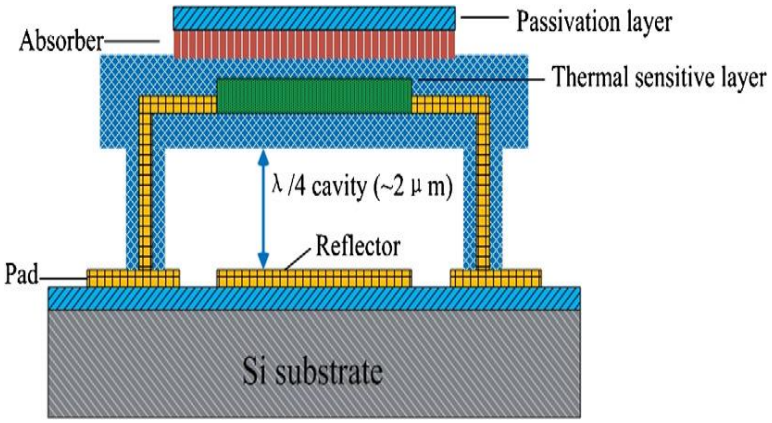

Figure 1.8: The structure of the designed microbolometer[23].

I.4.6. Micro-Fabrication Process

Thermal bolometric detectors can be fabricated on thermally isolated hanging membranes by utilizing micro-electro-mechanical systems (MEMS) technology [29] by this following stapes:

- A thin film with thickness of 250 nm, which play role of reflector, was sputtered and patterned by photolithography on 300 nm of silicon nitride layer.
- Polyimide, which acts as sacrificial layer, was spin coated. This is to pattern and make the anchor areas.
- Silicon nitride (350nm) and silicon dioxide (200nm) were deposited by Plasma Enhanced Chemical Vapour Deposition (PECVD); the contact holes were etched to be open by Reactive Ion Etching (RIE).
- After formation of the contact holes, Cr/Au electrodes with thickness of 10 nm/80nm respectively were deposited for electrical connection,electrodes areas were patterned to connect bottom pad. The electrodes were of very low resistivity and good adhesion.
- Vanadium oxide thin film with thickness of **100 nm** was deposited and patterned by ion beam sputtering for thermal sensitive material.
- Silicon dioxide (100 nm) and silicon nitride (100 nm) were deposited by PECVD again, which material act as insulation layer between TiN and VOx.
- TiN layerwith sheet resistance of 376 Ω and thickness of 60 nm was deposited by sputtering, which material acts as absorbing layer.
- Another silicon nitride with thickness of 200 nm was deposited to act as passivation layer.
- Finally, removal of polyimide sacrificial layer was finished by plasma asher in oxygen atmosphere[30].

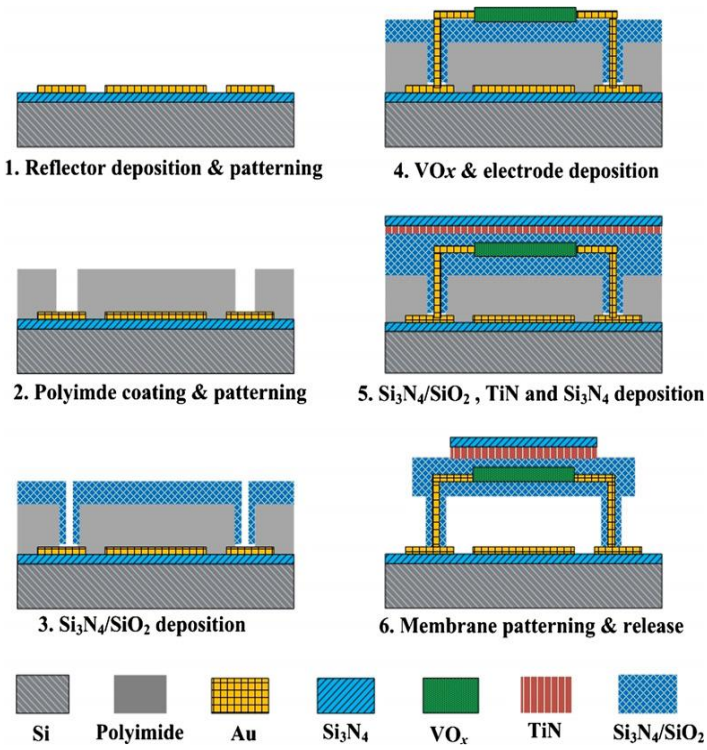

Figure 1.9: Schematic diagram showing the processes of microbolometer suspended structure[23].

I.5.State of The Art

Due to the development of MEMS technology, uncooled infrared bolometers have now maintained the performance levels of cooled infrared photon detectors. The performance of a thermal detector can be divided into two steps [31]:

Raising the temperature of a sensing material by input radiation and using the temperature dependent variation of a particular property of the material as its response.

The second step is involving the use of material property, depends on the type of thermal detector and, for a bolometer, TCR is utilised. TCR is related to the voltage responsivity, a widely used parameter to specify the performance of a bolometer, as [32] :

$$R_V = \frac{I_b R \alpha \eta}{G\sqrt{1+\omega^2\tau^2}} \qquad (1)$$

Where:

$\mathbf{R_v}$ Voltage responsivity.

$\mathbf{I_b}$ The bias current.

$\boldsymbol{R}$ the electrical resistance.

$\boldsymbol{\alpha}$ the temperature coefficient of resistance (TCR) , with TCR = (1/R)*dR/dT.

$\boldsymbol{\eta}$ the absorptivity of the VO*x* films.

$\boldsymbol{G}$ the thermal conductance of the suspended structure.

$\boldsymbol{\omega}$ the modulation frequency set by the mechanical chopper.

$\boldsymbol{\tau}$ the thermal time constant equal to $\boldsymbol{C/G}$, where $\boldsymbol{C}$ is the thermal mass of the isolated structure.

The TCR value of a specific material can be obtained experimentally by measuring the slope of the variation of the film resistivity with the temperature, which is described by the expression[33].

$$TCR = 1/R(dR/dT) \quad (2)$$

The complete characterisation of a microbolometer requires the understanding of both electrical and optical properties. The bolometer consists of a sensing element as VOx having a strong temperature coefficient of resistance TCR so that a small temperature change caused by the incident radiation it can be measured [34]. Usually, vanadium oxide thin film for microbolometer has TCR that ranges from 2% to 3% at room temperature. However, high TCR vanadium oxide thin film of 6.5%/K has been achieved by growing mixed phases of VO_2 and V_2O_3 with the method of reactive ion sputtering [35]. To promote microbolometer sensitivity, the improvement of TCR of thermal sensitive material is an important way, while it's necessary to consider whether the preparation of this material is compatible with CMOS for bolometer [23]. In addition to TCR, the films resistance should be tuned in a manner to avoid high 1/f noise even if, according to the relation (1), R_v increases by increasing the resistance. However, high films resistance leads to high 1/f noise and high TCR. This is shown is **Figure 1.10** where TCR is plotted versus the resistivity at 300°K [36]. Accordingly, one has to find the best balance between the resistivity and the TCR. It has been a common agreement that suitable VOx thin films for bolometer applications must have resistivity below 10 Ωcm with a TCR near 2%/K [37].

Figure 1.10 shows also the discrepancy between data obtained from different techniques of films deposition. The pulsed DC VOx does not compare favourably with ion beam sputtered VOx which is considered as a dominant method for producing microbolometer-quality VOx for use in infrared imaging devices [38]. Due to the lack of overlap between the two populations of samples, it is clear there must be a microstructural or chemical difference between the two leading to the discrepancy. Microstructurally, the most obvious difference between the two sets of data is the morphology of the nano-crystalline phase. In ion beam sputtered films, there is a tendency for the nano-crystalline phase to grow in high-aspect ratio columns throughout the thickness of the film, whereas the pulsed DC films typically exhibit more equiaxed particles [35-36].

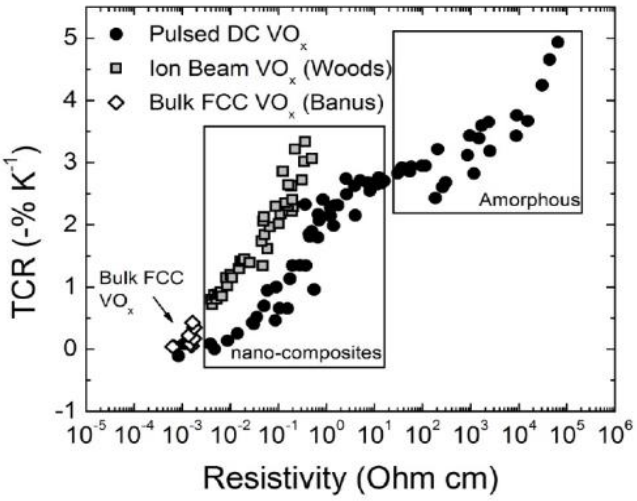

Figure1.10: The resistivity at 300°K vs TCR plot of pulsed DC data including regions denoting microstructural character. Included in the plot is ion beam data from reference [39] and bulk FCC VOx data from reference [36].

The work presented in last year [40] , deals the development and study of the Properties of vanadium oxide thin films. They used thermal evaporation for 50mg of V_2O_5 powder, and annealing process at different time (t= 5 min, 10min, 15min, 20min, 25min, 30min, 60min, 90min) at T°=(400°C, 450°C, 500°C). From the results of experience, they concluded that it is impossible to obtain only VO_2 in the same thin film by using the thermal evaporation technique and annealing process but it is possible to obtain a mixture of VOx.

Our study will be based on the effect of thickness on the electrical properties of thin VOx films, we chose the sample of 400°C annealing temperature for 5 min due to its higher TCR

(2,58 %/°K). This relatively high TCR value was compatible with high films resistivity (136 Ohm.cm). It is therefore necessary to find the right thickness, which makes it possible to have a large TCR and an acceptable resistivity. This is what we want to achieve by using the VOx thin films. It was reported that 65–200 nm film thickness is usually chosen for bolometer applications [41] and an optimal films thickness can be found within this range of thickness [42].

I.6.Conclusion

The fascinating properties and broad applications of vanadium oxide have attracted considerable interest. The optical and electrical properties of vanadium oxide thin films are sensitive to temperature, which made it possible to be integrated within a category of materials for microbolometer application.

CHAPTER II

Thin Films Generalities

II.1.Introduction

The ever-increasing integration of devices, especially in the field of microelectronics, requires the development of increasingly sophisticated deposition techniques for the elaboration of materials in the form of thin layers. After a presentation of definitions and mechanisms of formation of thin films, we focus on some of the most used methods to obtain VOx oxide in the form of thin layers , and also the thin film characterization method.

II.2.Definition of thin layer

A thin film is a layer of material ranging from fractions of a nanometer (monolayer) to several micrometers in thickness. The controlled synthesis of materials as thin films (a process referred to as deposition) is a fundamental step in many applications[43].

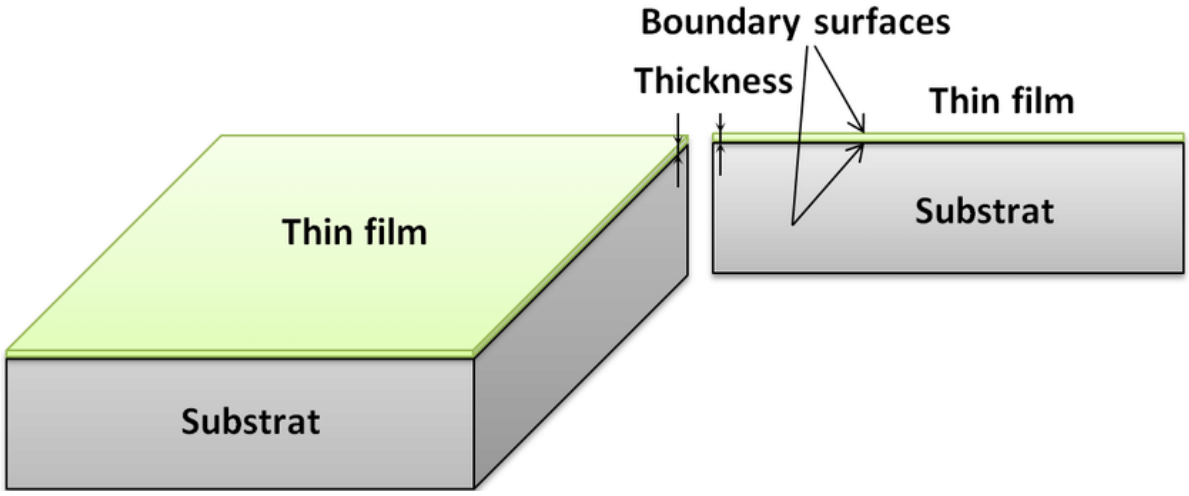

Figure2.1: Schematic of thin film deposited on a glass substrate [44].

II.3.Thin films deposition precedure

Thin film deposition is the technology of applying a very thin film of material – between a few nanometers to about 100 micrometers, onto a "substrate" surface to be coated, or onto a previously deposited coating to form layers. Thin film deposition manufacturing processes are at the heart of today's semiconductor industry, solar panels, CDs, disk drives, and optical devices industries.

Thin Film Deposition is usually divided into two broad categories – Chemical Deposition and Physical Vapor Deposition Coating Systems.

Physical Vapor Deposition refers to a wide range of technologies where a material is released from a source and deposited on a substrate using mechanical, electromechanical or thermodynamic processes. The two most common techniques of Physical Vapor Deposition or **PVD** are Thermal Evaporation and Sputtering [45].

II.3.1.Physical vapour deposition procedure (PVD)

PVD stands for Physical Vapor Deposition. PVD Coating refers to a variety of thin film deposition techniques where a solid material is vaporized in a vacuum environment and deposited on substrates as a pure material or alloy composition coating.

As the process transfers the coating material as a single atom or on the molecular level, it can provide extremely pure and high performance coatings which for many applications can be preferable to other methods used. At the heart of every microchip, and semiconductor device, durable protective film, optical lens, solar panel and many medical devices, PVD Coatings provide crucial performance attributes for the final product. Whether the coating needs to be extremely thin, pure, durable or clean, PVD provides the solution.

It is used in a wide variety of industries like optical applications ranging from eye glasses to self-cleaning tinted windows, photovoltaic applications for solar energy, device applications like computer chips, displays and communications as well as functional or decorative finishes, from durable hard protective films to brilliant gold, platinum or chrome plating.

The two most common Physical Vapor Deposition Coating processes are Sputtering and Thermal Evaporation. Sputtering involves the bombardment of the coating material known as the target with a high energy electrical charge causing it to "sputter" off atoms or molecules

that are deposited on a substrate like a silicon wafer or solar panel. Thermal Evaporation involves elevating a coating material to the boiling point in a high vacuum environment causing a vapor stream to rise in the vacuum chamber and then condense on the substrate[45].

II.3.2.Atomic Layer Deposition

Atomic layer deposition involves self-limited surface reactions for the growth of metal oxide by sequentially exposing the surface to metal and oxygen sources one after the other. ALD of vanadium oxides was first studied for catalytic applications and for Li-ion batteries. In these cases, V_2O_5 was the phase of interest. V_2O_5 reported starting from vanadyl-tri(isopropoxide) precursor. Furthermore, post-deposition annealing of other vanadium oxide phases in air is expected to result in V_2O_5. In case of VO_2 the controlled reduction of the ALD grown V_2O_5 yields good quality films but the reduction conditions are often governed by very narrow operating conditions which makes VO_2 synthesis by ALD difficult. Nevertheless, considerable amount of research has been performed by the group of Detavernier at Ghent university and significant advances were reported for the growth of high quality VO_2 films by ALD using relatively new kind of precursors such as tetrakis ethyl methyl amino vanadium [TEMAV], tetrakis dimethyl amino vanadium, [TDMAV], and tetrakis diethyl amino vanadium [TDEAV] [46].

II.4.Characterization technique for deposited films

II.4.1.Stuctural and surface analyse

II.4.1.a.X-ray diffraction

The origin of X rays: In November 1895, Wilhelm Rontgen discovered X-rays while working at the University of Wurzburg, Germany. Rontgen was investigating cathode rays in different types of evacuated glass tubes and trying to determine their range in air. He noticed that while the rays were being produced, a screen coated in fluorescent barium platinocyanide would glow. He was intrigued because the screen was too far from the tube to be affected by the cathode rays. He assumed unknown rays, X-rays, were being emitted from the walls of the tube while the cathode ray tube was running. To his amazement, Rontgen found that the rays could pass straight through his hand and cast shadows of his bones on the fluorescent screen. He spent several weeks privately investigating the rays before publishing his results at the end

of the year. Rontgen's paper described many of the properties of X-rays. He showed that they were:

- Very penetrating and were able to pass through materials that are opaque to visible light.

- Invisible to the human eye.

- Would cause many types of material to fluoresce and could be recorded

on photographic paper.

They were named 'rays' because they moved in straight lines like visible light.

II.4.1.a.1 : Using X-rays as an analytical tool: The Bragg father and son duo explained that an X-ray which reflects from the surface of a substance has travelled less distance than an X-ray which reflects from a plane of atoms inside the crystal. The penetrating X-ray travels down to the internal layer, reflects, and travels back over the same distance before being back at the surface. The distance travelled depends on the separation of the layers and the angle at which the X-ray entered the material. For this wave to be in phase with the wave which reflected from the surface it needs to have travelled a whole number of wavelengths while inside the material. Bragg expressed this in an equation now known as Bragg's Law:

$$n\lambda = 2d \sin\theta$$

When λ is the wavelength of the X-ray, n is an integer (1, 2, 3 etc.) The reflected waves from different layers are perfectly in phase with each other and produce a bright point on a piece of photographic film. d is the interatomic distance and the angle of diffraction is θ. A visual representation of Bragg's law is shown in figure2.4 The x-ray diffraction pattern of a pure substance is, therefore, like a fingerprint of the substance. The powder diffraction method is thus ideally suited for characterization and identification of polycrystalline phases[46].

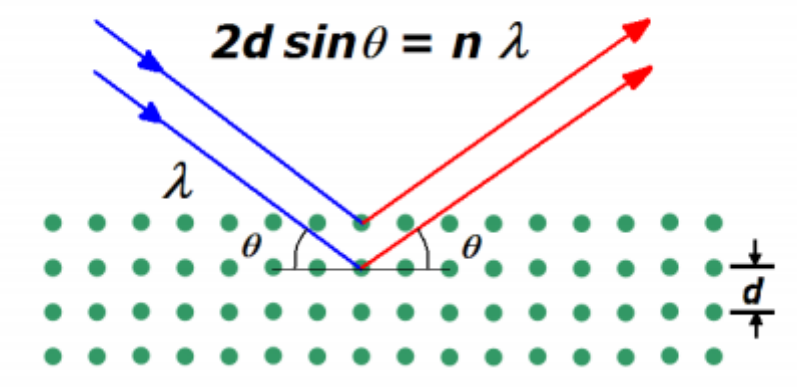

Figure2.2 : A schematic representation of Bragg's law[46].

X-ray diffractometers consist of three basic elements: an X-ray tube, a sample holder, and an X-ray detector. In a typical X-ray diffraction instrument, X-rays are generated in a cathode ray tube by heating a filament to produce electrons, accelerating the electrons toward a target by applying a voltage, and bombarding the target material with electrons. When electrons have sufficient energy to dislodge inner shell electrons of the target material, characteristic X-ray spectra are produced. These spectra consist of several components, the most common being Kα and Kβ. Kα consists, in part, of Kα1 and Kα2. Kα1 has a slightly shorter wavelength and twice the intensity as Kα2. The specific wavelengths are characteristic of the target material (Cu, Fe, Mo, Cr). Filtering, by foils or crystal monochrometers, is required to produce monochromatic X-rays needed for diffraction. Kα1and Kα2 are sufficiently close in wavelength such that a weighted average of the two is often used. Copper is the most common target material for single-crystal diffraction, with CuKα radiation = 1.5418Å. These X-rays are collimated and directed onto the sample. As the sample and detector are rotated, the intensity of the reflected X-rays is recorded. When the geometry of the incident X-rays impinging the sample satisfies the Bragg Equation, constructive interference occurs and a peak in intensity occurs. A detector records and processes this X-ray signal and converts the signal to a count rate which is then output to a device. The geometry of an X-ray diffractometer as shown in figure.2.5 a is such that the sample rotates in the path of the collimated X-ray beam at an angle θ while the X-ray detector is mounted on an arm to collect the diffracted X-rays and rotates at an angle of 2θ. The instrument used to maintain the angle

and rotate the sample is termed a goniometer. Within the scope of the current study of Vanadium oxide films XRD technique plays a vital role in determining whether the as grown films feature a pure, or mixed phase oxides[46].

II.4.1.a.2 : Grazing incidence X-Ray diffraction : the angle of incidence a (angle between the incident beam and the surface) is fixed and of low value. By varying the angle of the detector (the only element in rotation during the analysis), the entire spectrum is collected. Experiences X-ray diffraction tests were using a Philips X'Pert PRO type diffractometer. The X-ray source used is the Koc radiation from a copper anticathode (X = 0.154 056 nm)[47].

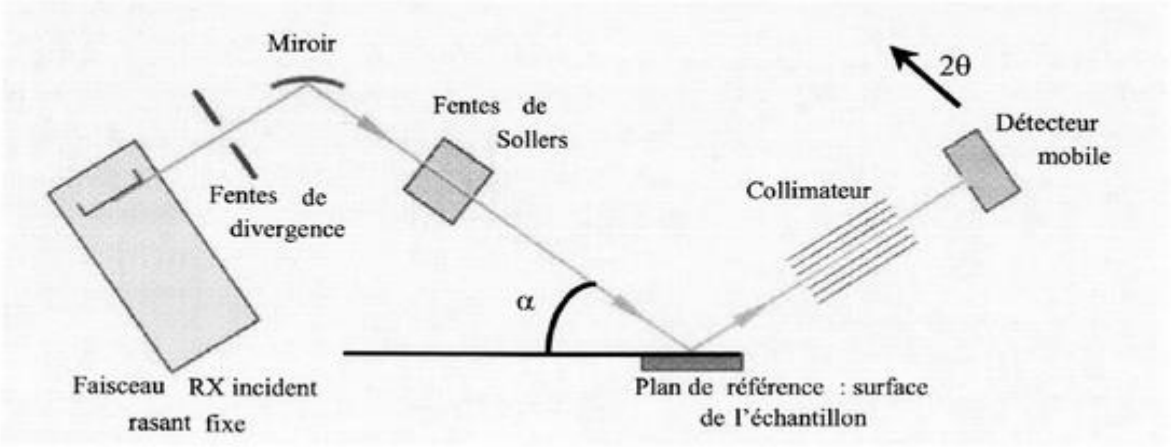

Figure2.3: Configuration of
grazing incidence X-ray diffraction setup [47].

II.4.1.b.Scanning Electron Microscope (SEM)

The scanning electron microscope (SEM) uses a focused beam of high-energy electrons to scan the surface. This electron beam is produced at the top of the column, accelerated downward and passed through a combination of lenses and apertures to the sample. The sample is mounted on a stage in the chamber area and, both the column and the chamber are evacuated by a combination of pumps. **Figure.2.4** (a) and (b) shows the schematic and photographic image of a scanning electron microscope.

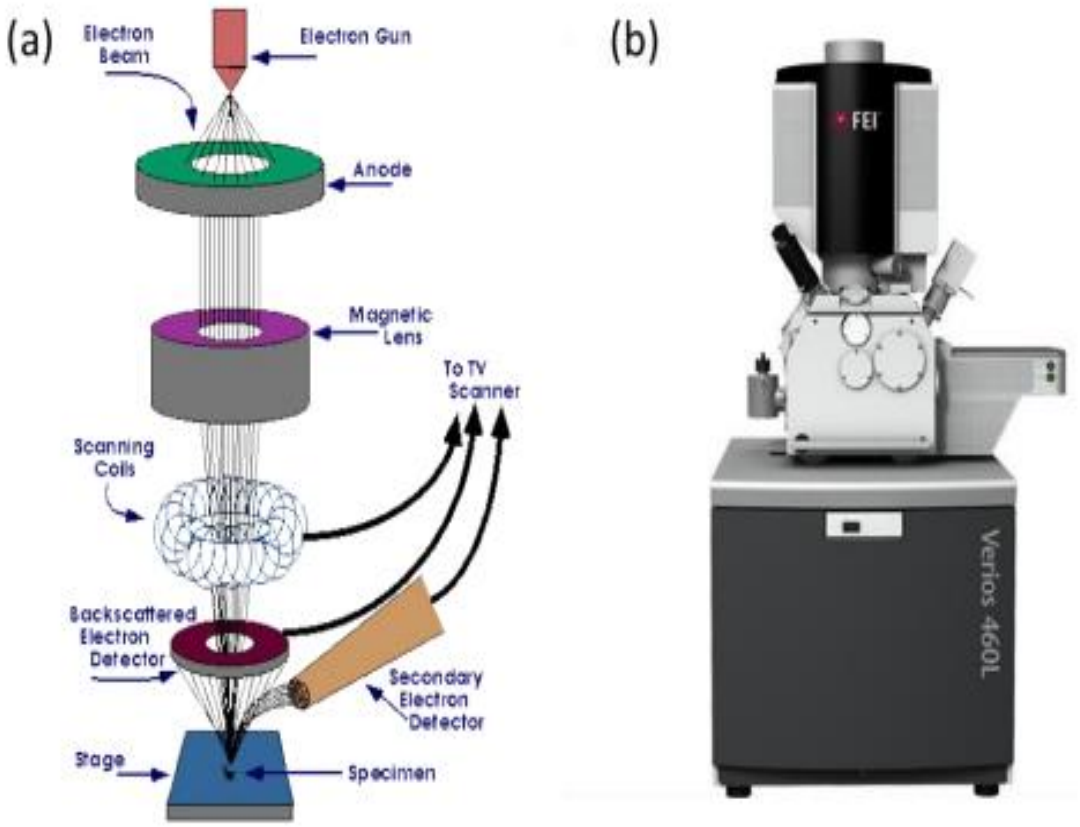

Figure2.4: Detailed schematic of the working principle of a scanning electron microscope and (b) a photographic image of the SEM used for analysis in this study [46].

The signals that derive from beam-sample interactions reveal information about the sample including external morphology (texture), chemical composition, and crystalline structure and orientation of materials making up the sample. In most applicatons, data are collected over a selected area of the surface of the sample, and a 2-dimensional image is generated that displays spatial variations in these properties. Areas ranging from approximately 1 cm to 5 microns in width can be imaged in a scanning mode using conventional SEM techniques. An example of surface and cross section SEM images are shown in Figure2.9. Here two different morphologies are observed as a result of growing the films with two distinct precursor concentrations. Such morphological information is crucial in determining the final properties of thin films.

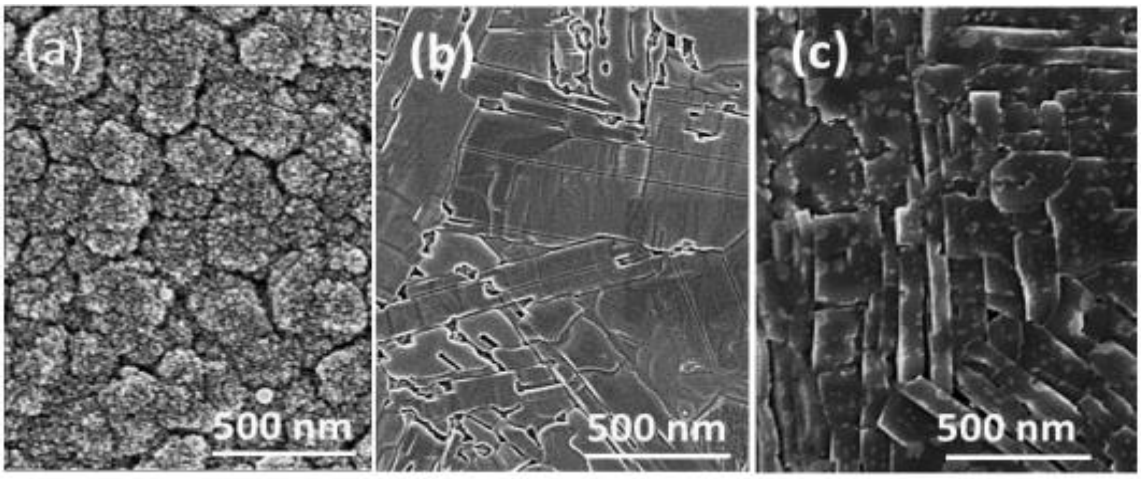

Figure2.5 : Surface SEM micrographs of the as deposited VO_X film (a) with a nanocrystalline morphology. (b) & (c) show the surface micrographs of V_2O_5 and VO_2 formed after oxidation and reduction treatments respectively[46].

II.4.2. Morphology and thickness analysis

II.4.2.a : Profilometer Device

A profilometer is a measuring instrument used to measure a surface's profile, in order to quantify its roughness. Critical dimensions as step, curvature, flatness are computed from the surface topography.

While the historical notion of a profilometer was a device similar to a phonograph that measures a surface as the surface is moved relative to the contact profilometer's stylus, this notion is changing with the emergence of numerous non-contact profilometry techniques.

Non-scanning technologies are able to measure the surface topography within a single camera acquisition, XYZ scanning is no longer needed. As a consequence, dynamic changes of topography are measured in real-time. Contemporary profilometers are not only measuring static topography, but now also dynamic topography – such systems are described as time-resolved profilometers.

Types :

Optical methods[48-49] include interferometry based methods such as digital holographic microscopy, vertical scanning interferometry/white light interferometry, phase shifting interferometry, and differential interference contrast microscopy (Nomarski microscopy);

ocus detection methods such as intensity detection, focus variation, differential detection, critical angle method, astigmatic method, foucault method, and confocal microscopy; pattern projection methods such as Fringe projection, Fourier profilometry, Moire, and pattern reflection methods.

Contact and pseudo-contact methods[48-49] include stylus profilometer (mechanical profilometer)[50] atomic force microscopy[51], and scanning tunneling microscopy.

II.4.3.Electrical properties analysis

II.4.3.a : Four-pointed technique :

Four-terminal sensing (4T sensing), 4-wire sensing, or 4-point probes method is an electrical impedance measuring technique that uses separate pairs of current-carrying and voltage-sensing electrodes to make more accurate measurements than the simpler and more usual two-terminal (2T) sensing. Four-terminal sensing is used in some ohmmeters and impedance analyzers, and in wiring for strain gauges and resistance thermometers. Four-point probes are also used to measure sheet resistance of thin films (particularly semiconductor thin films)[52].

Separation of current and voltage electrodes eliminates the lead and contact resistance from the measurement. This is an advantage for precise measurement of low resistance values. For example, an LCR bridge instruction manual recommends the four-terminal technique for accurate measurement of resistance below 100 ohms[53].

Four-terminal sensing is also known as Kelvin sensing, after William Thomson, Lord Kelvin, who invented the Kelvin bridge in 1861 to measure very low resistances using four-terminal sensing. Each two-wire connection can be called a Kelvin connection. A pair of contacts that is designed to connect a force-and-sense pair to a single terminal or lead simultaneously is called a Kelvin contact. A clip, often a crocodile clip, that connects a force-and-sense pair (typically one to each jaw) is called a Kelvin clip[54].

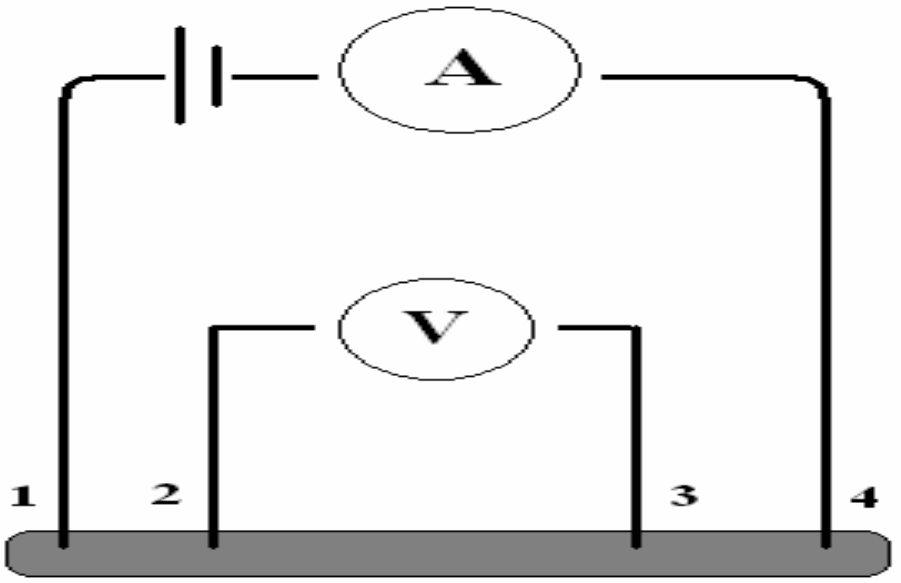

Figure2.6 : Four-point measurement of resistance between voltage sense connections 2 and 3. Current is supplied via force connections 1 and 4 [55].

II.5.Experimental Procedure

During our experiment, the technique of vacuum thermal evaporation was used to deposit the thin layers, we used a Vanadium pentoxide powder with a purity of 99.6 %.

II.5.1.Nature of Substrate

We chose two kinds of slides, Glass (1mm thick and 25x75 mm 2 of surface) and Silicon (110) slide because of theirs naturals properties, the glass is an amorphous, insulating, transparent, chemically inert solids materials and silicon is an polyoptic and resistif to a higher temperatures, both are a candidate for bolometer applications [56]. Samples that have glass as a substrate were used to determine structural and electrical properties, and samples that have silicon as substrate were used to determine morphological structure such as the thin film's thickness measure.

II.5.2. Preparation of Substrate

The quality of the deposit and consequently that of the sample depends on the Cleanliness and condition of the substrate. Cleaning is therefore a very important step, all traces of grease and dust must be removed. These conditions are essential for the proper adhesion of the deposit on the substrate, and for its uniformity (constant thickness). The process of cleaning the surface of substrates is as follows:

- The substrates are cut with a diamond tip pen.
- Degreasing in an acetone bath for 5 minutes.
- Washing in ethanol at room temperature in an Ultrasonic bath to remove traces of grease and impurities attached to the surface of the substrate for 5 minutes.
- Drying with compressed air.
- Put the substrates on a hot plate so that the rest of the ethanol evaporates.

II.5.3.The Deposition Procedure

Before starting each experiment, we wait until a sufficient vacuum is reached within the chamber. First, we start the primary pumping until we reach a pressure of about 1.10 -2 mbar, then we start the secondary pumping until around 10 -5 mbar, the deposition procedure will be carried out under a temperature exceeding 1400°C and a voltage of 200V. After the Vacuuming of the enclosure, the material will be evaporated using a crucible electrically heated by joule effect and finally the steam will condense on the substrates. The main parameters used to develop vanadium oxide layers are summarized in Table 2.1:

Table II.1: The main deposition parameters of VOx films.

V2O5 powder mass (mg)	Primary pressure (mbar)	Work's pressure (mbar)	Secondary pressure (mbar)	Deposit time (s)
70	1,6.10-2	2,7.10-4	2,1.10-5	19
50	1,87.10-2	1,4.10-4	2,85.10-5	20
25	1,5.10-2	1,2.10-4	3,5.10-5	25
15	1,75.10-2	1,1.10-4	2,0.10-5	34

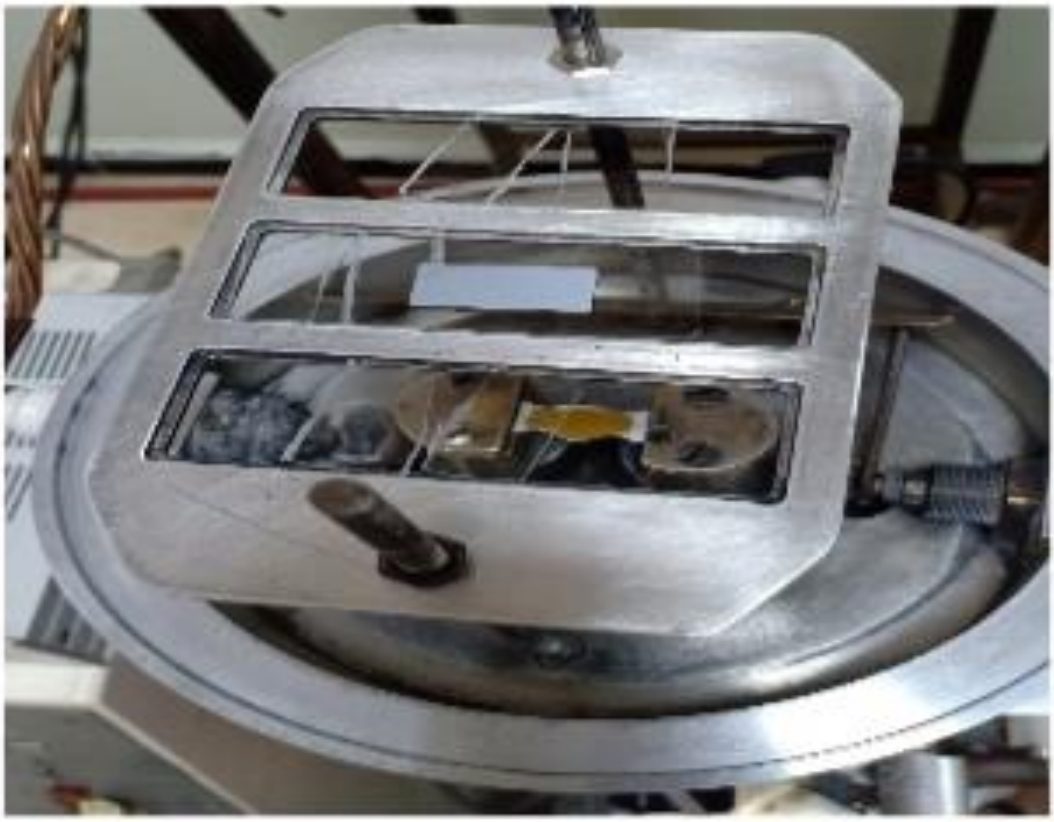

Figure2.7 : The deposition method of VOx thin layers in a vacuum chamber(CDTA).

II.5.4. Annealing Procedure

After deposition, the samples have undergone an electrical and morphological and structural study then underwent an annealing heat treatment to carry out a second study, in an oven powered by 130W power, under an atmosphere at temperature of 400°C for 5min,the temperature is measured by a REG48 Thermo Regulator witch is an instrument for controlling temperature. The temperature regulator takes an input from a temperature sensor, and has an output that is connected to a control element, such as a heater. To control the process temperature accurately, without significant intervention by the operator, the temperature control system relies on a real-time regulator that accepts a temperature sensor as input such as a thermocouple. It compares the actual temperature to the desired control temperature, or set point, and provides an output to a control element.The temperature regulator is part of the complete control system, and the entire system must be analysed when selecting the corresponding temperature regulator.

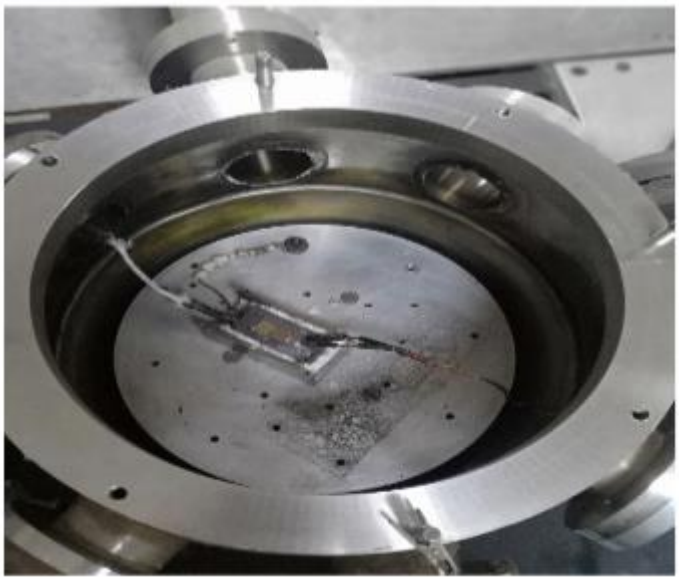

Figure2.8 : Photograph of the annealing device (CDTA).

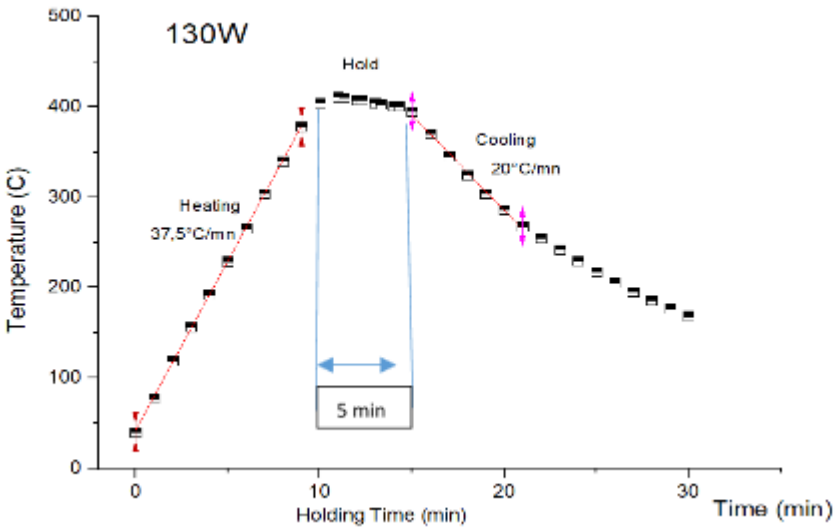

Figure2.9: Annealing Process treatment.

Figure2.9 show the annealing process treatment, the oven heats up for 10 min by 37,5°C/min ,until it reaches 400 ° C and then it stabilizes at this temperature for 5 min to perform the annealing conditions (400 ° C for 5 min) then the temperature decreases for 10 min by 20°C/min until it reaches the value of the ambient temperature even if it exceeds 10

minutes, the most important thing is that the annealing temperature is fixed constant during the whole annealing time.

- During our study, the purpose of annealing is to go from the amorphous state to the crystalline state by increasing the grain size of the composite material and carrying out a study of the properties of the material after annealing to be able to observe the difference of the different properties and especially the electrical behaviour before and after annealing.

II.6. Conclusion

We succeeded in depositing the thin layers of vanadium oxide by thermal vacuum evaporation. The annealing process allows the thin film to change from amorphous state to crystalline state.

The XRD and SEM techniques inform us about the crystallographic structure and the surface analysis. The profilometer technique allow us to measure the films thickness. Finally by using the four-point technique, we can define the electrical properties.

CHAPTER III
RESULTS AND DISCUSSIONS

III.1.Introduction

After realising vanadium oxide layers by thermal evaporation on substrates of glass and silicon, we will discuss the experimental results of the influence of thickness on the structural, morphological and electrical properties of the elaborated layers.

III.2.Surface Morphology

a) Thickness Measurements:

In order to measure the thickness by using the profilometer device,we carried out a deposit of the VOx thin films on highly polished silicon and glass substrates. The results were as following:

Table.III.1: VOx thin layers Thickness deposited on glass and Silicon substrates.

V_2O_5 mass (mg)	Thickness on Silicon substrate (nm)	Thickness on Glass substrate (nm)
70	191	210
50	150	201
25	95	163
15	56	47

Table.III.1 Shows the measurement of the thickness of thin VOx layers on a glass and silicon substrate. We observe a nuance of difference on the results obtained due to the deformation of the glass, knowing that the glass is not resistive to temperature (here we are talking about the deposit temperature which exceeded 1400° C), for this the results obtained on silicon substrate are the most reliable.

Table.III.1 hows the evolution of thin layers thickness deposited on Silicon substrate versus the V_2O_5 evaporated mass. The films thickness increases from 56 nm to 191 nm when the evaporated mass increases from 15 mg to 70 mg.

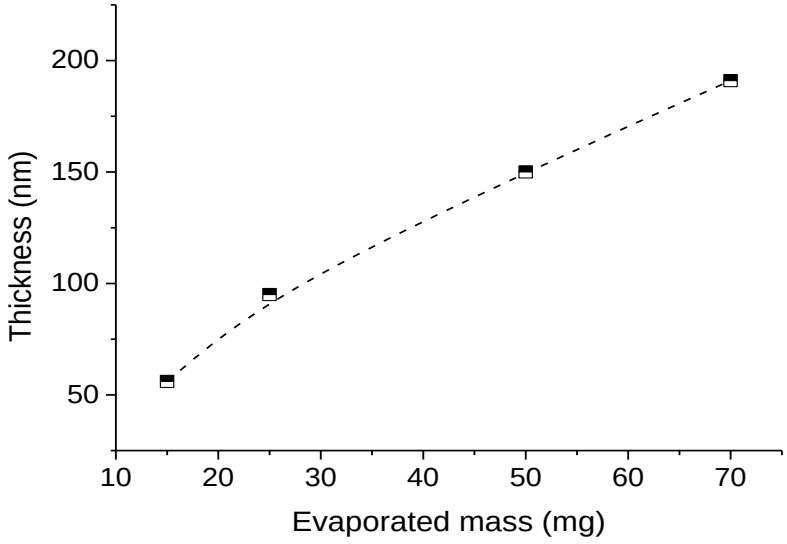

Figure 3.1: Films thickness versus the evaporated mass. The dashed line is a guide to the eye.

b) Surface Morphology:

We used SEM (Scanning Electron Microscopy) to obtain a microscopic image of different annealed thin layers. Blistering or buckling driven delamination of thin films that forms blisters can be seen. This effect is caused by a large compressive stress in thin films, probably due to a thermal mismatch origin between the substrate and the film. Buckling is a problem common to many materials after thermal treatments as reported by Malerba et al. [57] and is essentially a mechanical instability which causes the film to develop large out-of-plane displacement above a critical limit [58]. This limit depends on the temperature, the morphology of oxide layer, the cooling rate and the thickness [59]. Considering this latter and in our case, by increasing the films thickness the diameter of the blisters increases and their density decreases. Further, the microstructure of the 191 nm thick film seems to be more developed as the grains are more apparent.

-series 70mg:

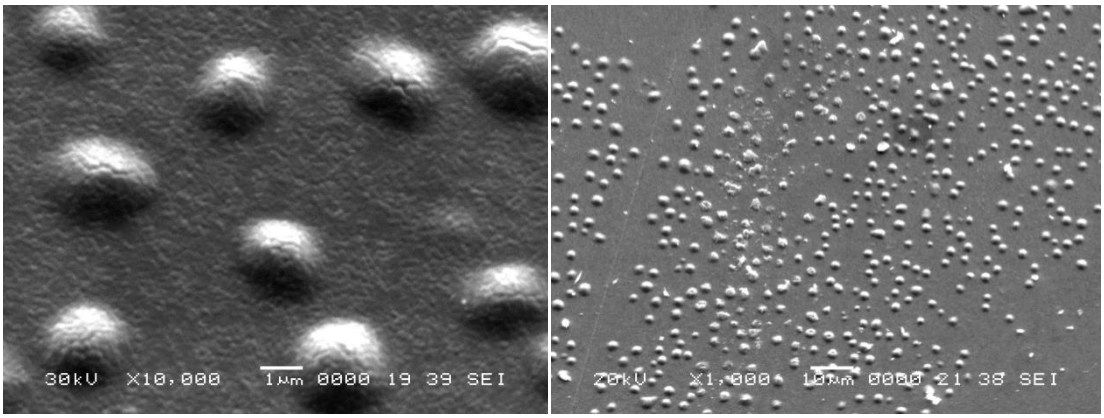

Figure3.2: SEM image of evaporated and annealed VOx thin layer (70 mg).

-Series 50mg:

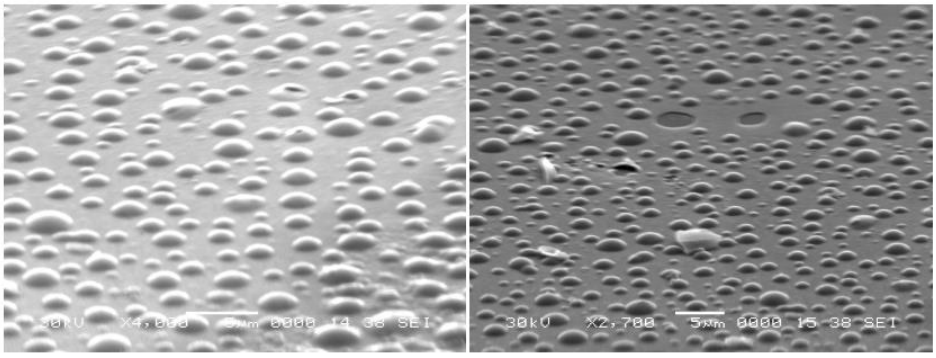

Figure3.3: SEM image of evaporated and annealed VOx thin layer (50mg).

-Series 25mg:

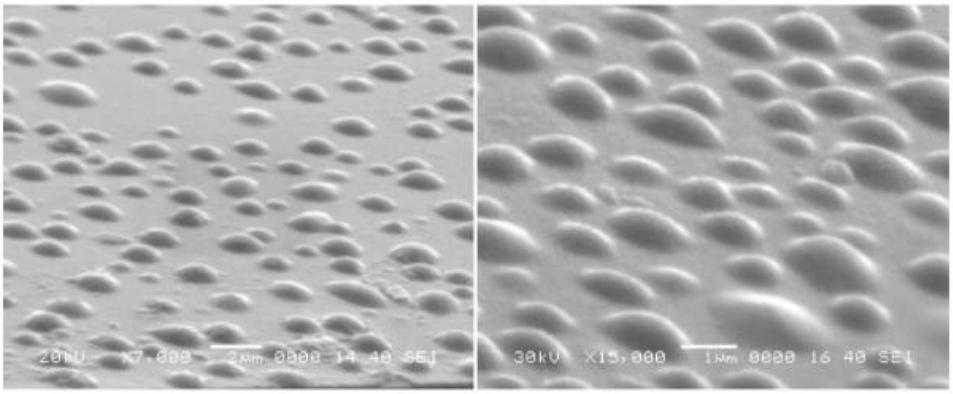

Figure3.4: SEM Image of evaporated and annealed VOx thin layer (25mg).

-Series 15mg:

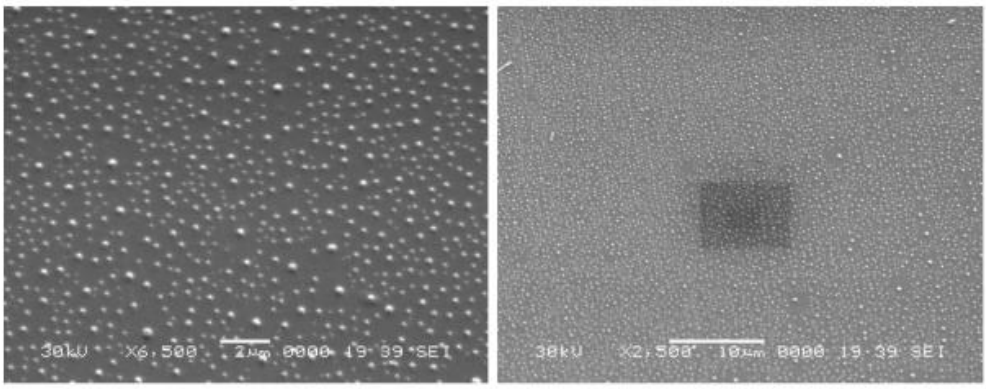

Figure 3.5: SEM Image of evaporated and annealed VOx thin layer (15mg).

III.3.structural analysis

Figures 3.6 shows the grazing XRD patterns of as-deposited and annealed VOx thin films. While the as-deposited films are amorphous (figure 3.6-a), the annealed films are crystalline (figure 3.6-b).

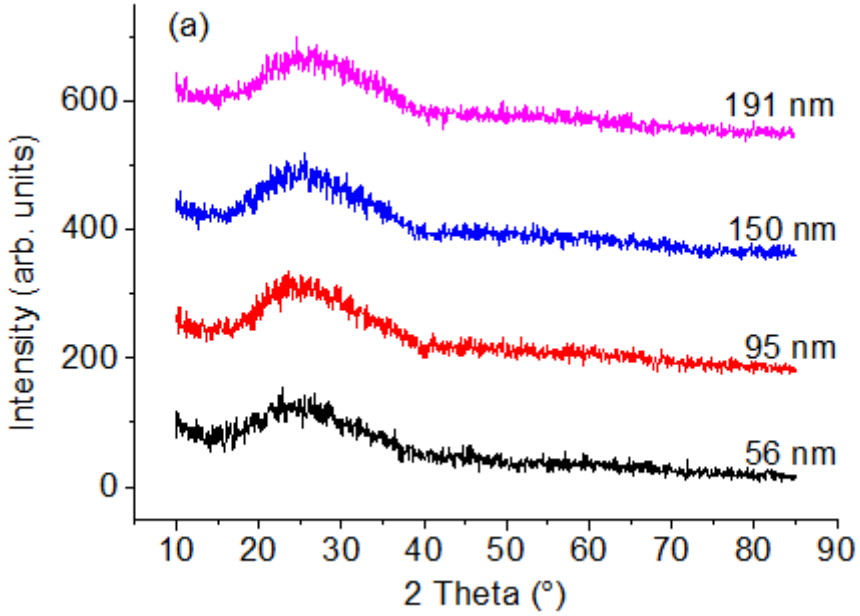

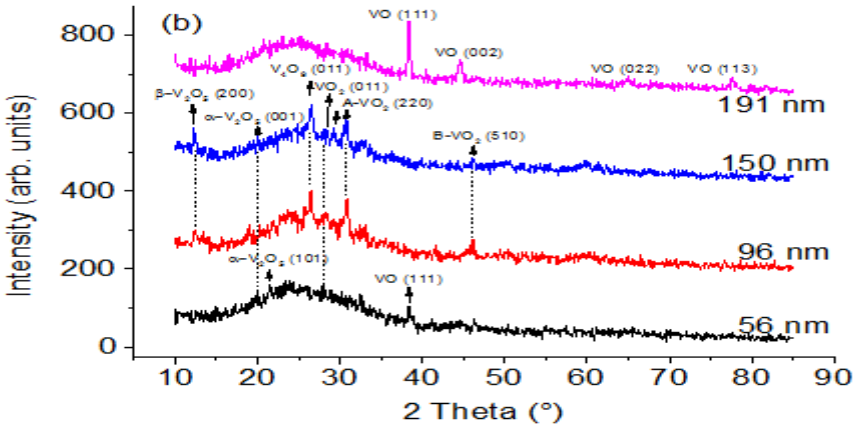

Figure 3.6: Grazing XRD patterns of as-deposited and annealed VOx thin films.

A preliminarily identification of the crystalline phases has revealed the following:

- 56 nm thick films contain VO_2 (A and M phases), V_2O_5 (α phase) and VO as a dominant phase.

- 96 nm thick films contain V_4O_9, VO_2 (M and B phases) with V_4O_9 as a dominant phase.

- 150 nm thick films contain V_4O_9, VO_2 (M, B and A phases) and V_2O_5 (α and β phases) with V_4O_9 as dominant phase.

- 190 nm thick films contain only VO phase.

Accordingly, the growth of VO phase is favored at low and high thickness, while at intermediary thicknesses, V_4O_9 is dominant with the presence of VO_2 phase.

III.4.Electrical Measurement

Deposited and annealed vanadium oxide thin films of different thickness were electrically characterised using 4 points method.

III.4.1. Resistance Measurement

In the first place, we measured the resistance of each sample of each series, we obtained these following results:

-Series 70mg:

Table.III.2: Resistance Measurement of 191 nm films thickness.

Sample's number	1 (Glass)	2 (Glass)	3 (Glass)	4 (Glass)	5 (Si)
Resistance(Kohm)	198	220	170	167	88

-Series 50mg:

Table.III.3: Resistance Measurement of 150 nm films thickness.

Sample's number	1 (Glass)	2 (Glass)	3 (Glass)	4 (Glass)	5 (Glass)	6 (Si)
Resistance(Mohm)	0,42	0,86	0,86	0,74	0,57	0,072

-Series 25mg:

Table.III.4: Resistance Measurement of 95 nm films thickness.

Sample's number	1 (Glass)	2 (Glass)	3 (Glass)	4 (Glass)	5 (Si)
Resistance(Mohm)	0,8	1,2	1,1	0,94	0,8

-Series 15mg:

Table.III.5: Resistance Measurement of 56 nm films thickness.

Sample's number	1 (Glass)	2 (Glass)	3 (Glass)	4 (Glass)	5 (Glass)	6 (Si)
Resistance(Mohm)	1,94	2	2,2	3	2,45	0,040

These tables show the resistance measurement of each series. We obtained different values of resistance. Our choice was based on the homogeneity of the samples before each electrical characterisation.

III.4.2. V-I Characteristics

At room temperature, an (I-V) measurement was set up for each sample chosen to confirm Ohm's law by confirming the linearity of the (I-V) graph.

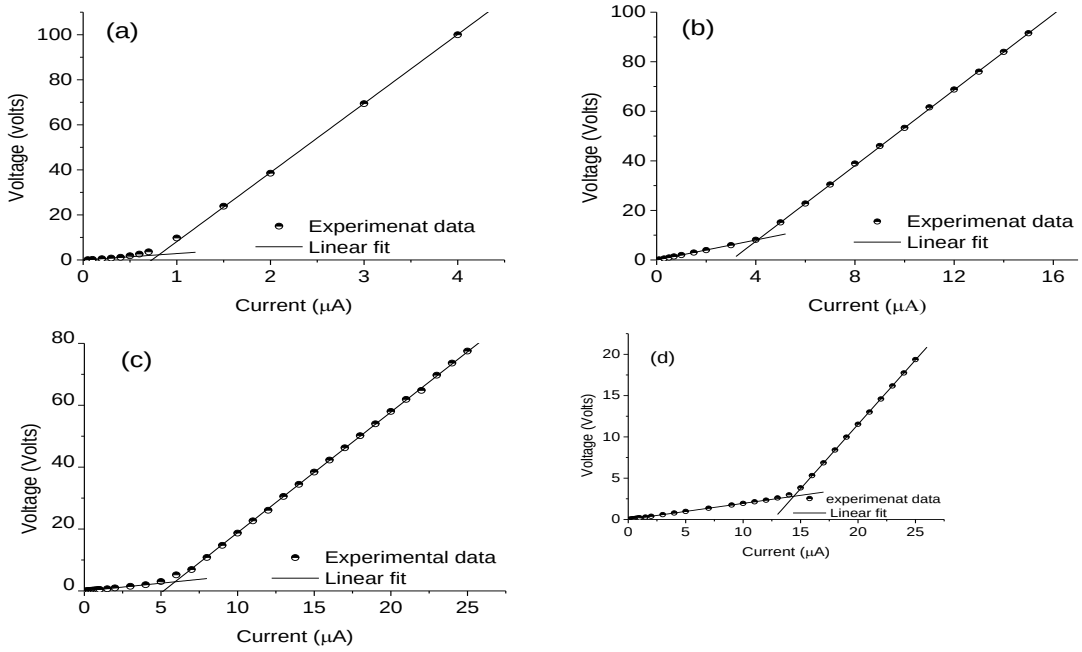

Figure 3.7: (V-I) Characteristics of as-deposited VOx thin films at different thickness:

(a) 56nm, (b) 95 nm , (c) 150nm, (d) 191nm.

Figure 3.7 shows the V-I characteristics of as-deposited VOx thin films at different thickness. When we observe the figures, we notice that there is a kind of transition in the electrical conductivity of VOx thin films at different values of bias current depending on the thickness.

- In **figure 3.7 (a)** for **56 nm**, the first interval of linearity has been observed from [0 µA to 0,7µA] , then the transition was carried out at 1 µA.
- In **figure 3.7 (b)** for **95nm**, the first interval of linearity has been observed from [0 µA to 4 µA] then the transition was carried out at 5 µA.
- In **figure 3.7 (c)** for **150 nm**, the first interval of linearity has been observed from [0 µA to 5 µA] , then the transition was carried out at 6 µA.
- In **figure 3.7 (d)** for **191 nm**, the first interval of linearity has been observed from
- [0µA to 14 µA], then the transition was carried out at 15 µA.

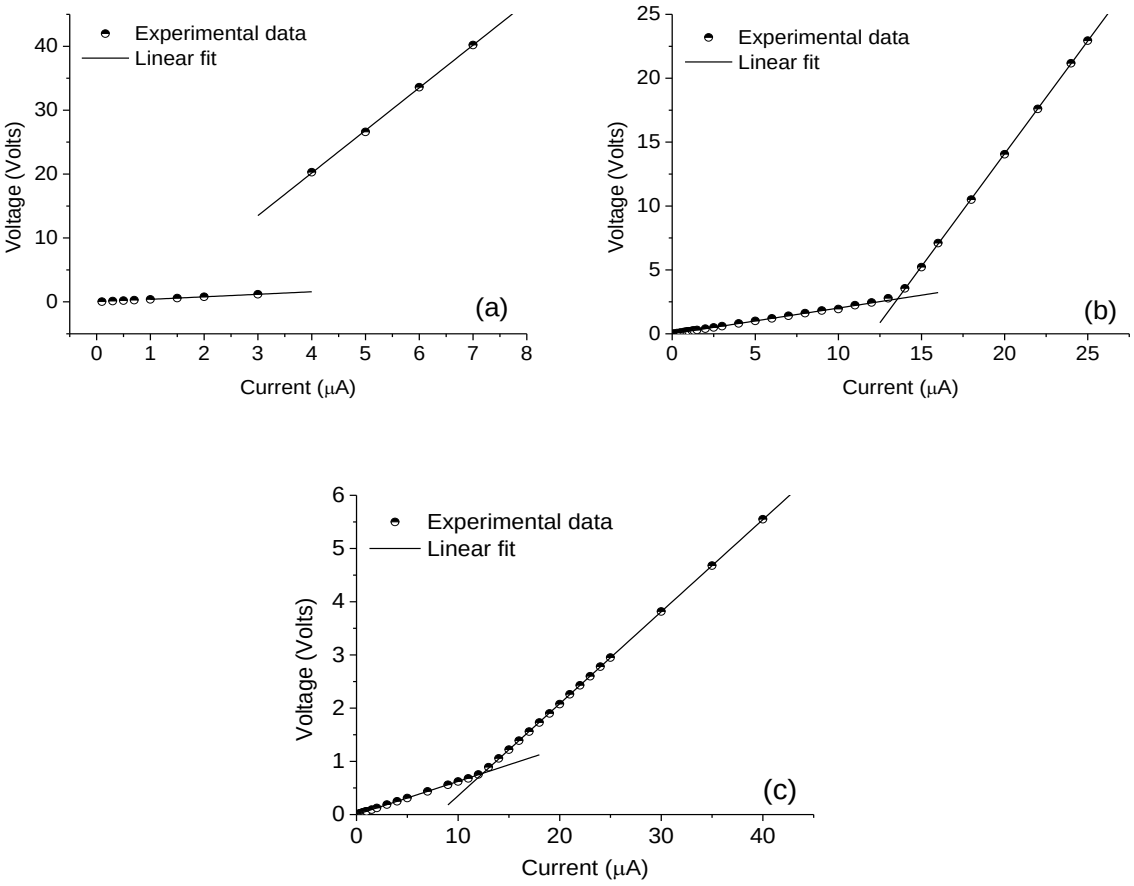

Figure 3.8: (V-I) Characteristics of annealed VOx thin films with different thickness:

(a) 95 nm, (b) 150 nm, (c) 191 nm.

Figure 3.8 shows the V-I characteristics of annealed VOx thin films at different thickness. As for as-deposited films, we observed a transition in the conductivity behaviour at different values of bias current as fellow:

- In **figure 3.8 (a)** for **95nm**, the first interval of linearity has been observed from [0 µA to 3 µA], then the transition was carried out at 4 µA.
- In **figure 3.8 (b)** for **150 nm**, the first interval of linearity has been observed from [0µA to 13 µA], then the transition was carried out at 14 µA.
- In **figure 3.8 (c)** for **191 nm**, the first interval of linearity has been observed from [0µA to 14 µA], then the transition was carried out at 15 µA.

- **Note:** After annealing, the sample of thickness of 56 nm has not undergone an (V-I) characteristic, because of the phenomenon of agglomeration which appears during annealing process where holes grow until the film is transformed into a collection of unconnected grains which are electrically isolated [60]. This caused a large increase in resistance which exceeded 200 MΩ, knowing that our device is limited to this value.
- **Observation:** Making a small comparison (figure 3.8), we observe that the threshold bias current of the conductivity transition increases when the thickness increases for both as-deposited and annealed films. While samples of thickness of 95 nm and 191 nm kept its current threshold path before and after annealing, there is a change for the sample of 150 nm thickness.

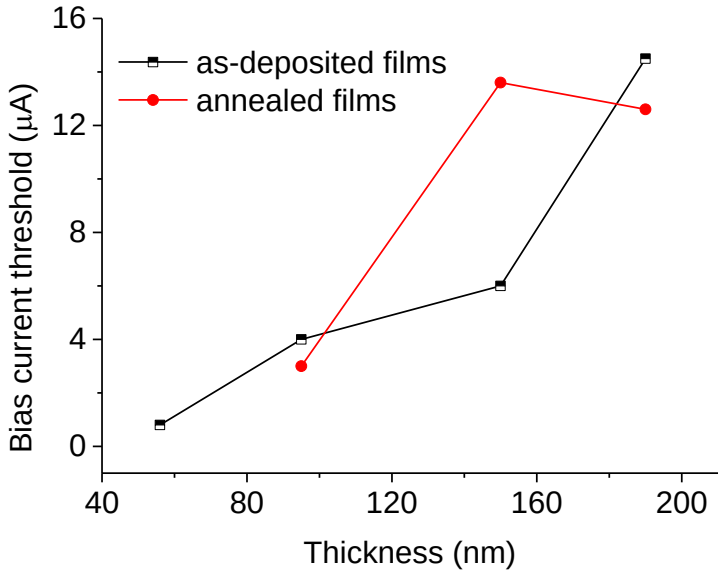

Figure3.9: Bias Current threshold versus films thickness.

We think that the bias current dependent conductivity behaviour is due to phases competing in VOx films throughout the films thickness.

III.4.3. Temperature dependence of Resistivity

In this section, we will present the effect of temperature on a-deposited and annealed VOx films resistance and the effect of thickness on electrical resistivity.

a) Electrical properties stabilisation upon multiple thermal cycling:

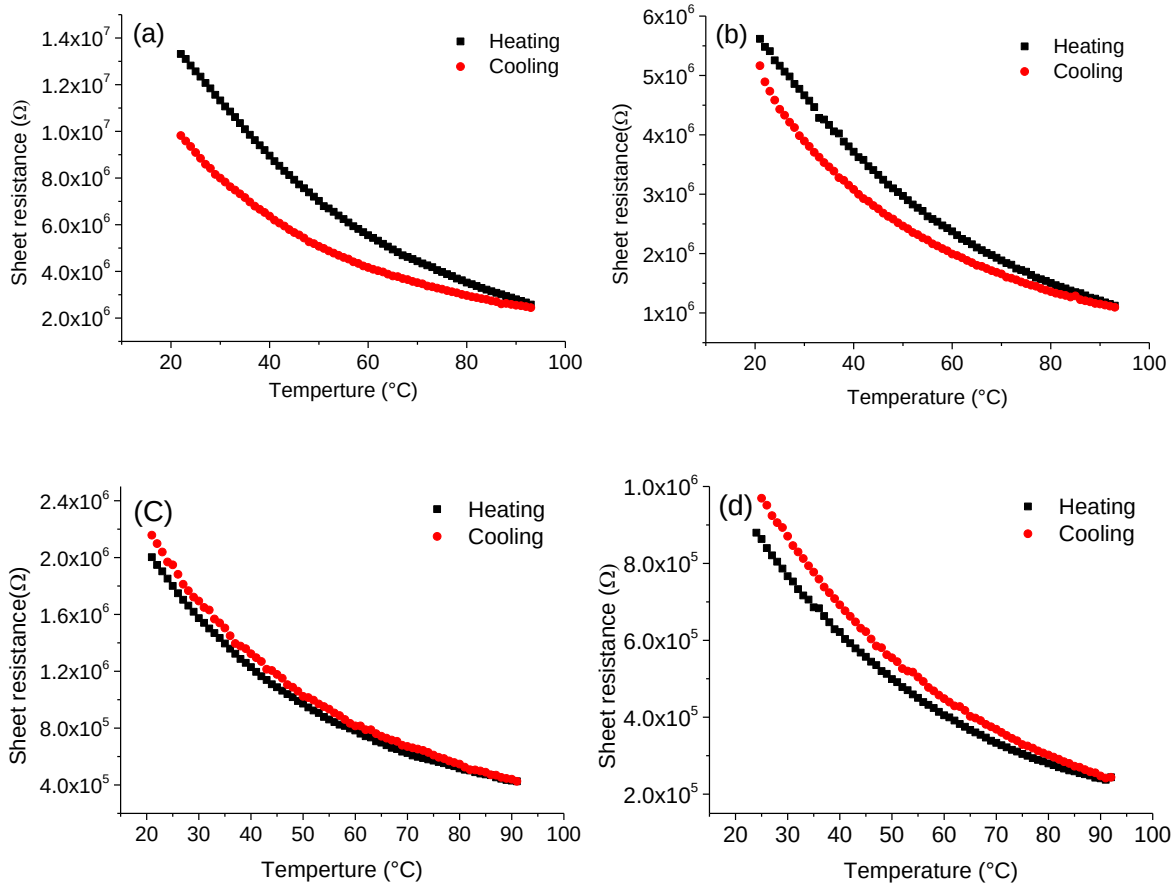

Figure 3.10: Sheet Resistance of as-deposited VOx thin films upon first thermal cycling : **(a)** 56nm**, (b)** 95nm, **(c)** 150nm, **(d)** 191nm. The bias current is 0,5 µA.

Figure 3.10 Shows the first thermal cycling of different thin layers. The sheet resistance (*R*) versus the temperature (*T*) of the films doesn't undergo an hysteresis loop (it has not undergone the same path during heating and cooling). This effect is more accentuated at lower films thickness (**Figure 3.10 (a)**), while the 150 nm thick films shows an optimal *R*-*T* path (**Figure 3.10 (c)**).

To more understanding the thermal cycling, we have carried out a multiple cycles for the samples of 191 nm and 150 nm. **Figure 3.11** shows the different thermal cycles of samples of 150 nm and 190 nm thickness. According to the graphs, it is observed that the samples follow the same path during heating and cooling after having undergone some cycles that we think due to the stored strain relaxation.

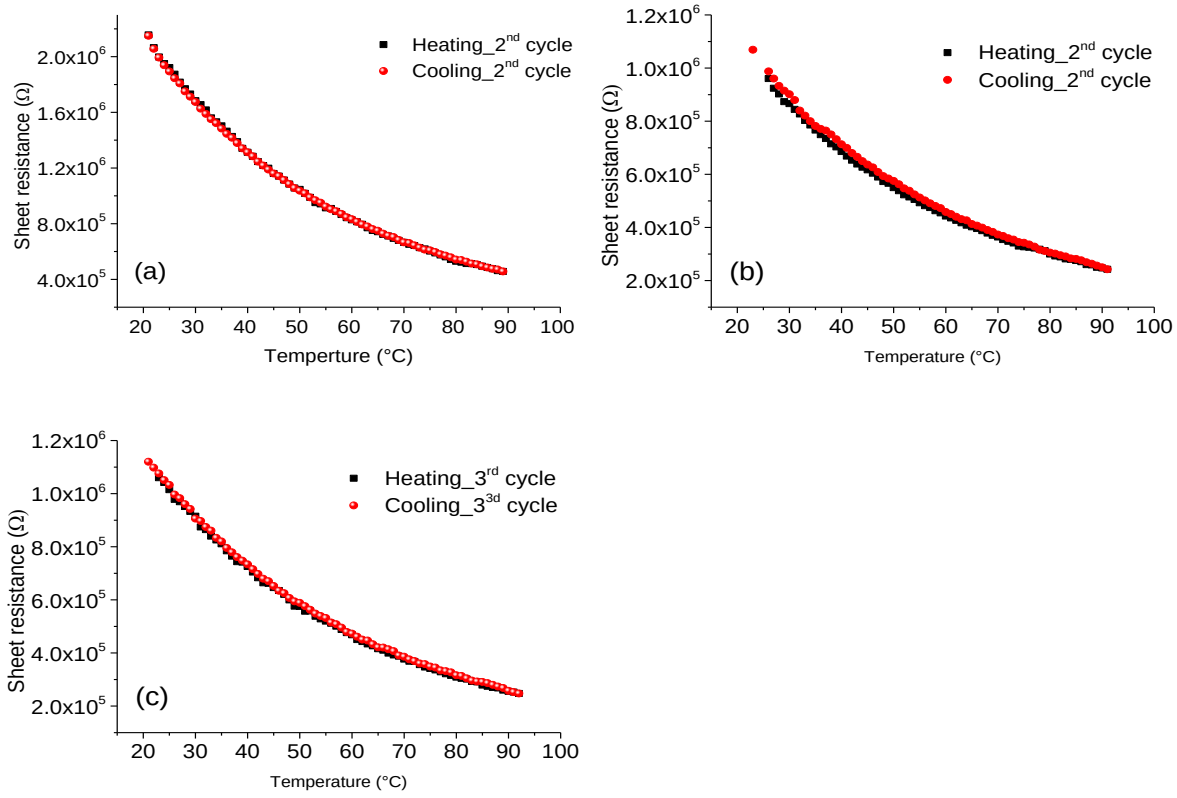

Figure 3.11: Sheet Resistance of as deposited VOx thin films upon multiple thermal cycling : (a) 150 nm under 2nd cycle, (b) 190 nm under 2nd cycle and (c) 190 nm under 3rd cycle. The bias current is 0,5 µA.

A typical behaviour of sheet Resistance upon multiple thermal cycling of the annealed VOx thin films thickness of 191 nm is presented in **figure 3.12**. According to the graph, we can observe that the sheet resistance does not take the same path during the first. From the second cycle, the sheet resistance started to take the same path. We notice a larger deviation of the sheet resistance of the annealed films during the first heating and cooling processes when comparing the as-deposited ones. This could confirm that this deviation is due to the stored strain as annealing process induce generally a large strain in the thin films.

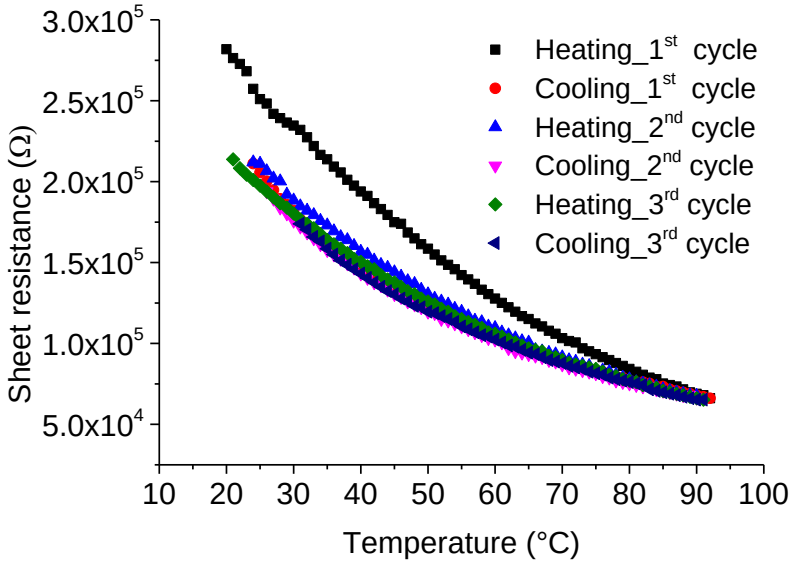

Figure 3.12: Typical sheet Resistance behaviour of annealed VOx thin films upon multiple thermal cycling. The thickness of the film is 190 nm.

b) Effect of the Thickness on the electrical Resistivity:

The electrical resistivity measurements at room temperature (300°K) of as-deposited and annealed VOx thin films are given in **figure 3.13**. The data presented in the latter figure are those obtained from the stabilised resistance versus temperature curves.

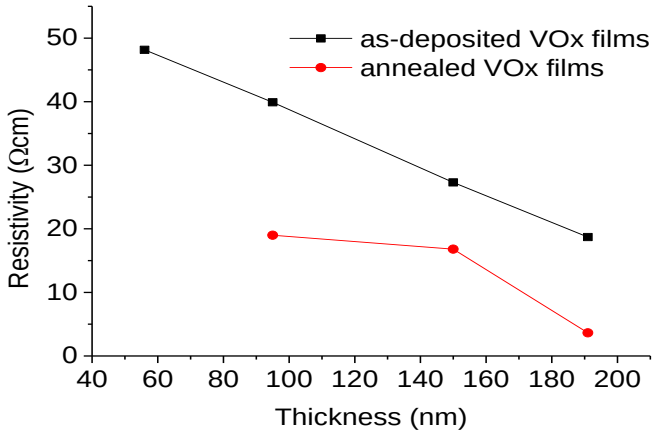

Figure 3.13. Electrical resistivity at room temperature (300°K) of as-deposited and annealed VOx thin films.

According to the **Figure 3.13** for the annealed and deposited thin layers, we observe the increasing of resistivity when the thickness decreases and vice versa. Further the annealing process reduces considerably the resistivity down to 3.6 Ωcm for the annealed 196 nm thick films due to the microstructural development as has been observed in the microscopic images.

III.4.4. Temperature coefficient of resistance (TCR) Measurement

In this section, we highlight the dependence of the TCR to the thickness and the bias current.

a) Thickness dependence of the temperature coefficient of resistance (TCR):

For each different thickness, we performed TCR measurements using the resistance versus temperature data. The bias current was 0.5 µA.

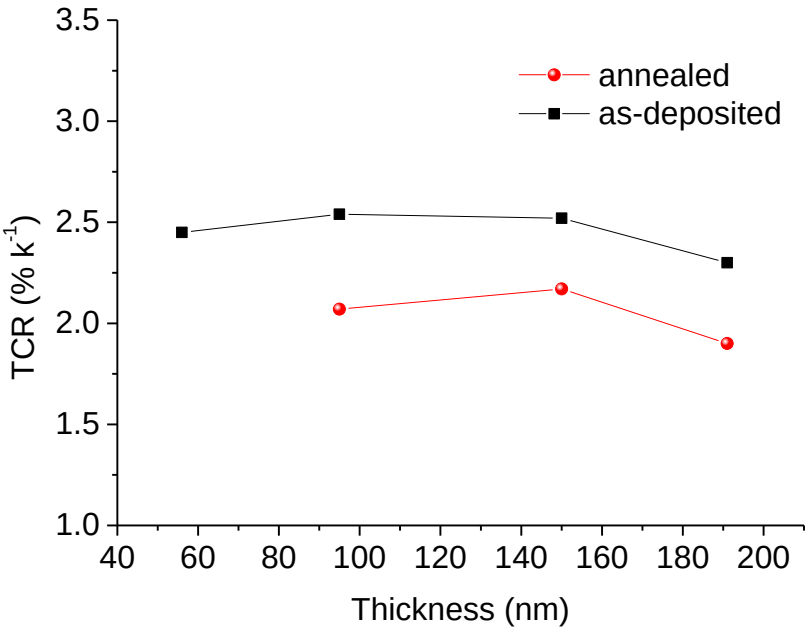

Figure 3.14. Thickness dependence of the temperature coefficient of resistance (TCR) at room temperature.

Figure 3.14 shows change of TCR according to the thickness. TCR does not change too much with thickness but it changes after annealing. The TCR is around 2.5 % K^{-1} for the layers as deposited and 2 % K^{-1} for the layers that have undergone annealing. This is no connection in TCR with a wide range of thickness has been reported by Nishikawa *et al*. [61]

B) Bias current dependence of the temperature coefficient of resistance (TCR):

For this study we chose 191 nm thick film for its low resistivity. This study was motivated by the observation of different resistances of the samples in different intervals of current.

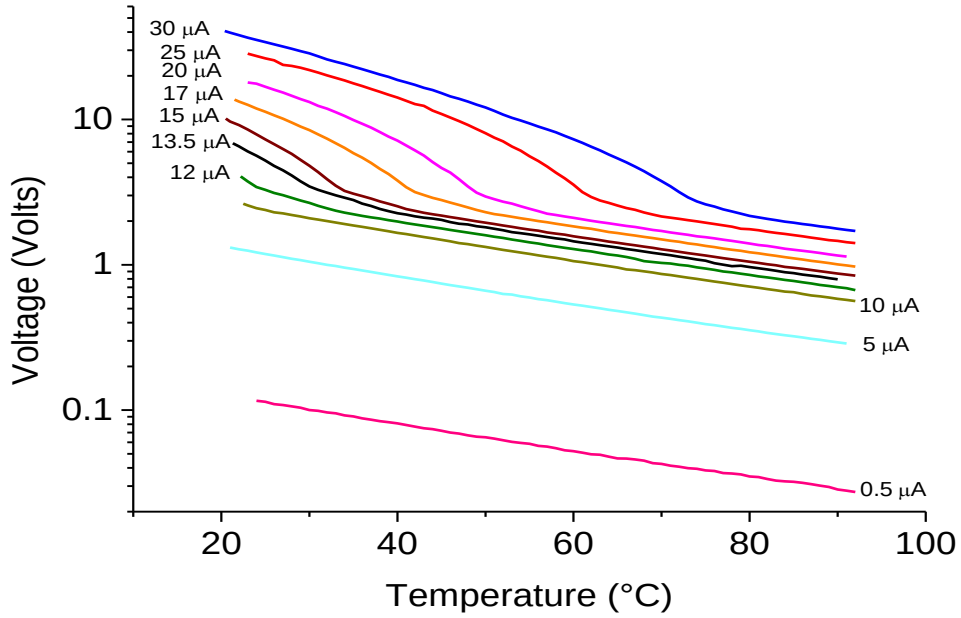

Figure 3.15: Bias current dependent voltage-temperature characteristics of as-deposited 191 nm thick films.

Figure 3.15 Shows the behaviour of the measured voltage depending on the temperature at different bias current. By changing the current in the first linear part of the V-I characteristics, in the range 0.5 - 10 µA, voltage-temperature characteristics shows a same behaviour. In the second linear part of the V-I characteristics, in the current range of 12 - 30 µA, two kinds of behaviour appears separated by a threshold temperature. This latter increases by increasing the bias current. Before the threshold temperature, the voltage drops fastly. Beyond the temperature threshold, the voltage-temperature behaviour resembles to that of the low currents. This confirms phases competing in our VOx thin films to impose the electrical properties. Low bias currents or high temperatures favour the phase with a low resistivity, while high bias current and low temperature favours the phase of high resistivity. If one consider the shape of the V-T curves and the dependence of the threshold temperatures to the bias current, one can conclude

that the later phase is VO_2. This can be confirmed by the hysteresis loop presented in **figure 3.16**.

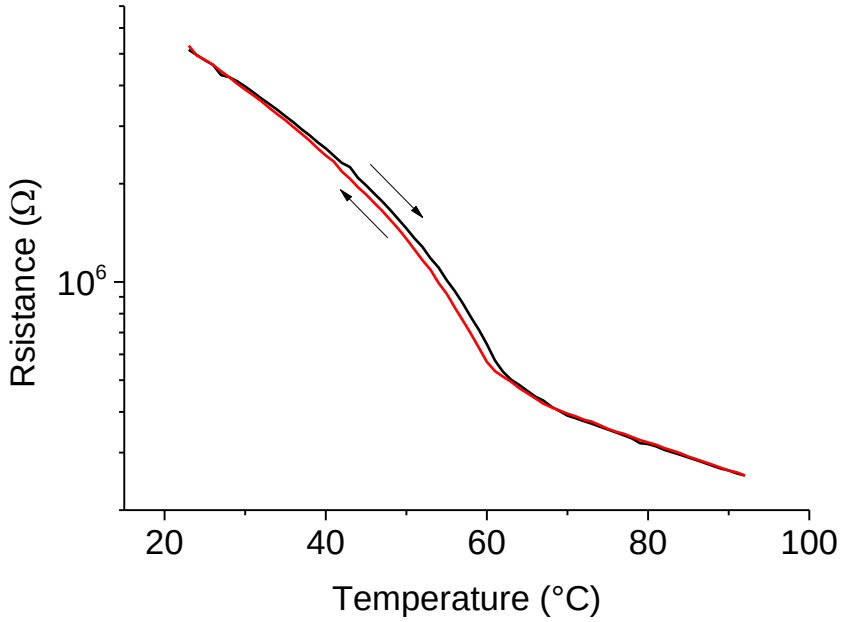

Figure 3.16: Hysteresis loop of As-deposited 191 nm thick films resistance versus temperature at bias current of 25 µA.

Figure 3.17 Shows the bias current dependent TCR at Room temperature of 191 nm thick films. We notice that the TCR values remains stable around 2.4 % K^{-1} from 0.5 µA to 10 µA (first region of V-I linearity), and vary from 9 % K^{-1} down to 3.7 % K^{-1} in 12 - 20 µA current range (second V-I linearity). The obtained high value of TCR isa characteristics of VO_2 thin films [62]-[63]. This confirms our assumption about the presence of VO_2 phase in our thin films.

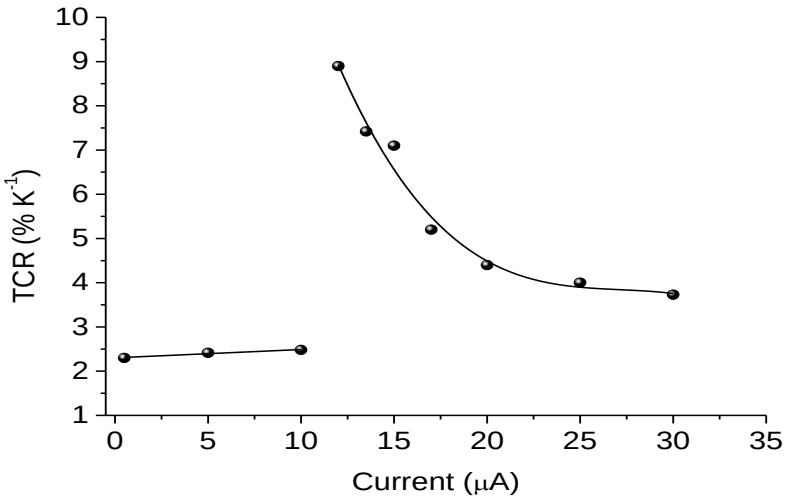

Figure 3.17: Bias current dependent TCR at room temperature of as-deposited 190 nm thick films.

Finally, **Figure 3.18** shows TCRs versus resistivities of this study. The thermal evaporation VOx films does not compare favorably with ion beam sputtered VOx [64] , which is a commonly used technique in the industry. For a given TCR, the thermal evaporation films resistivity is always higher. However, the thermal evaporation VOx films compare favorably with pulsed DC VOx films due to the microstructural resemblance [65].

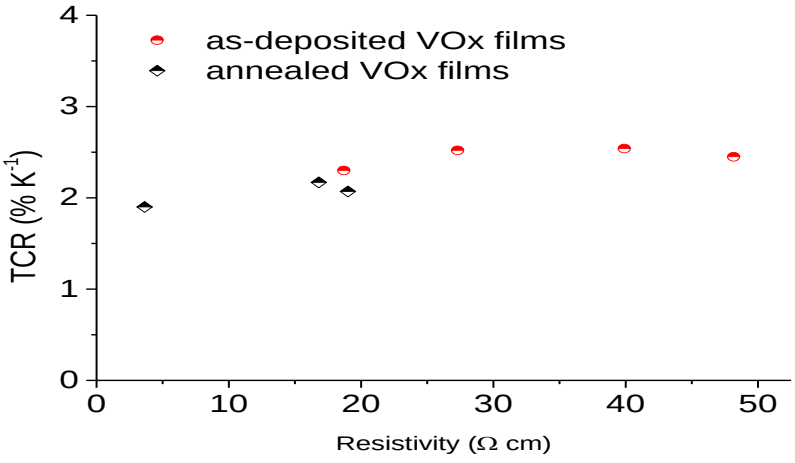

Figure 3.18: TCR versus resistivity of as-deposited and annealed VOx thin films.

III.5.Conclusion

The crystallization of VOx thin films through annealing process of thin films deposited by thermal evaporation technique was important for achieving a low resistivity and a common TCR value of 2 % K^{-1}. While the resistivity showed a high connection to the films thickness, TCR depends slightly on it. This gives a full potential for the realization of higher bolometric performance. Furthermore, using an appropriate bias current, the VOx thin films showed high TCR of 9 % K^{-1}. However, this performance is accompanied by a high resistivity (30 Ωcm). Concerning the microstructure, blistering appears to be a dominant feature that should be controlled in a perspective study. Further, deep analysis of the obtained VOx thin films by Hall effect measurement and depth-profiling X-ray photoelectron spectroscopy should give insights on the physico-chemical properties of these thin films. This will be very useful to trace a research plan for more bolometric performances.

GENERAL CONCLUSION

The work presented in this memory deals with the development and study of the properties of vanadium oxide thin films. To make these deposits, we used thermal evaporation from a V_2O_5 powder. This technique makes it possible to obtain deposits having properties depending on the development conditions. We then carried out heat treatments under air, to study their effects on composition and structure of thin layers made

The thickness of the VOx thin films is an evaporated mass dependence.
With the annealing process and in the range 56 - 191 nm, the films thickness control the phase evolution in VOx material. Low and high thickness favours a single phase formation (VO). Intermidiate thicknesses favour a Multiphase Vanadium Oxide thin Films formation.

The VOx microstructure is dominated by the blistering feature.

The crystallization of VOx thin films through the annealing process was important for achieving a low resistivity (3.6 Ωcm) and a common TCR value of 2 % K-1.

While the resistivity showed a high connection to the films thickness, TCR depends slightly on it.

By using an appropriate bias current, the VOx thin films showed high TCR of 9 % K-1 and non desirable high resistivity (30 Ωcm).

After studying all the characterizations of our films we can conclude that controlling the blistering and deep analysis of the obtained VOx thin films by Hall effect measurement and depth-profiling X-ray photoelectron spectroscopy.

Bibliographical references

[1] Louis Colombier, Gérard Fessier, Guy Henry, Joëlle Pontet, « Acier – Technologie », *Encyclopædia Universalis* [en ligne], (08 novembre 2020).

[2] David R. Lide, *CRC Handbook of Chemistry and Physics*, CRC Press Inc, (2009), 90e éd., 2804 p.

[3] Yi-Min Zhang , Shen-Xu Bao , Tao Liu , Tie-Jun Chen, Jing Huang The technology of extracting vanadium from stone coal in China: History, current status and future prospects, 9 May (2011).

[4] O'Neil, M.J. (ed.). The Merck Index - An Encyclopedia of Chemicals, Drugs, and Biologicals. Cambridge, UK: Royal Society of Chemistry, (2013)., p. 1840 .

[5] Haynes, W.M. (ed.). CRC Handbook of Chemistry and Physics. 95th Edition. CRC Press LLC, Boca Raton: FL (2014-2015), p. 4-40.

[6] Roger Molina, Propriétés chimiques de quelques composés du vanadium dans les chlorures alcalins fondus, Ecole de Physique et de Chimie, Paris (1961).

[7] D. Yin, N. Xu, J. Zhang, Xiulin Zheng. High quality vanadium dioxide films prepared by an inorganic sol-gel method.Materials Science (1996).

[8] Dernier, P. D. &Marezio, M. Crystal Structure of the Low-Temperature Antiferromagnetic Phase of V2O3. Phys. Rev. B 2, 3771–3776 (1970).

[9] Jayaraman, A., McWhan, D. B., Remeika, J. P. & Dernier, P. D. Critical Behavior of the Mott Transition in Cr-Doped V_2O_3. Phys. Rev. B 2, 3751–3756 (1970).

[10] Kuwamoto, H. &Honig, J. M. Electrical properties and structure of Cr-doped nonstoichiometric V_2O_3. J. Solid State Chem. 32, 335–342 (1980).

[11] Plowman SA, Smith DL. Exercise Physiology for Health, Fitness, and Performance. 4th ed. Philadelphia: Lippincott Williams & Wilkins; 2014. The Cardiovascular System; p.353.

[12] Metal-Insulator Phase Transition in Quasi-One-Dimensional VO 2 Structures - Scientific Figure on ResearchGate.crystal-structures-of-the-high-temperature-tetragonal-rutile-R-space- group_fig5_276921374 [accessed 8 Nov, 2020].

[13] Kokabi, H. R., Rapeaux, M., Aymami, J. A. &Desgardin, G. Electrical

characterization of PTC thermistor based on chromium doped vanadium sesquioxide. Mater. Sci. Eng. B 38, 80–89 (1996).

[14] Volker Eyert, The metal-insulator transitions of VO_2: A band theoretical approach , Institut für Physik, Universität Augsburg, 86135 Augsburg, Gemany,(23 October 2002).

[15] Metcalf, P. A. et al. Electrical, structural, and optical properties of Cr-doped and non-stoichiometric V_2O_3 thin films. Thin Solid Films 515, 3421–3425 (2007).

[16] Elizabeth E. Chain, Optical properties of vanadium dioxide and vanadium pentoxide thin films, (1 July 1991) / Vol. 30, No. 19 / APPLIED OPTICS, University of Texas at Dallas, Erik Jonsson,School of Engineering & Computer Science, P.O. Box 830688,

[17] H Yuce, H Alaboz, Y Demirhan, M Ozdemir, L Ozyuzer and G Aygun, Investigation of electron beam lithography effects on metal–insulator transition behaviour of vanadium dioxide, Department of Physics, Izmir Institute of Technology, 35430 Urla, Izmir, Turkey Teknoma Technological Materials Ltd, 35430 Urla, Izmir, Turkey (25 October 2017).

[18] Mansingh, A.; Singh, R.; Krupanidhi, S. B. Electrical Switching In Single Crystal VO_2. *Solid-State Electronics* 1980, *23* (6), 649–654.

[19] Pergament; Stefanovich; Kuldin; Velichko. On The Problem Of Metal-Insulator Transitions In Vanadium Oxides. *Isrn Condensed Matter Physics (*2013), *2013*, 1–6.

[20] Gupta A et al (2009) Semiconductor to metal transition characteristics of VO_2 thin films grown epitaxially on Si (001). Appl Phys Lett 95:111915.

[21] V. A. Klimov, I. O. Timofeeva, S. D. Khanin, F. Silva-Andrade.

TECH PHYS+ (Sep 2002) .

[22] Tissot J L (2004) Infrared Phys. Technol. 46 147.

[23] Bin Wang , Jianjun Lai , Hui Li , Haoming Hu , Sihai Chen , Nanostructured vanadium oxide thin film with high TCR at room temperature for Microbolometer, Wuhan National Laboratory for Optoelectronics, Wuhan 430074,School of Optoelectronic Science and Engineering, Huazhong University of Science and Technology, Wuhan 430074, China (2013).

[24] Rogalski A (2003) Infrared detectors: status and trends. Prog Quantum Electron 27:59–210.

[25] Venkatasubramanian C, Horn MW, Ashok S (2009) Ion implantation studies on VOx films prepared by pulsed dc reactive sputtering. Nucl Instrum Methods Phys Res Sect B 267(8–

9):1476–1479.

[26] Sedky S, Fiorini P, Caymax M, Baert C, Hermans L and Mertens R (1998) *IEEE Electron. Device Lett.* 19 376.

[27] Radford W *et al (*1996) *Proc. SPIE* 2746 82.

[28] O. Ozdemir, F. Gokdemir, U. Menda, P. Kavak, A. Saatci and K. Kutlu, "Nano-crystal V[sub 2]0[sub 5]nH[sub 2]0 sol-gel films made by dip coating", ‘(2012).

[29] Bhan RK et al (2009) Uncooled infrared microbolometer arrays and their characterisation techniques. Appl Opt 59:580–589.

[30] M.Klanjsek Gunde, M. Macek, Infrared optical constants and dielectric response functions of silicon nitride and oxynitride films, Basic Solid State Physics (a) 183 (2) (2001) 439–449.

[31] Niklaus F et al (2008) Performance model for uncooled infrared bolometer arrays and performance predictions of bolometers operating at atmospheric pressure. Infrared Phys Technol 51:168–177.

[32] R.T. Rajendra kumar, B. Karunagaran, D. Mangalaraj, Sa.K. Narayandass, P. Manoravi, M. Joseph, Vishnu Gopal et al., “Room temperature IR detection using pulsed laser deposited vanadium oxide bolometer”, International Conference on Smart Materials Structures and Systems (ISSS-SPIE 2002), India.

[33] Hernan M. R. Giannetta, Carlos Calaza, Liliana Fraigi and Luis Fonseca, Vanadium Oxide Thin Films Obtained by Thermal Annealing of Layers Deposited by RF Magnetron Sputtering at Room Temperature, in Modern Technologies for Creating the Thin-film Systems and Coatings, Edited by Nikolay Nikitenkov, IntechOpen, (2017).

[34] Niklaus F, Vieider C, Jakobsen H (2008) MEMS-based uncooled infrared bolometer arrays: a review. Proc SPIE 6836:68360D.

[35] Bin Wang, Jianjun Lai, Hui Li, Haoming Hu, Sihai Chen, Nanostructured vanadium oxide thin film with high TCR at room temperature for microbolometer, Infrared Physics & Technology 57 (2013) 8–13.

[36] Banus, M.D., T.B. Reed, and A.J. Strauss, Electrical and magnetic properties of TiO and VO. Physical Review B, (15 April 1972). 5(8): p. 2775 - 2784.

[37] H. Alaboz, Y. Demirhan, H. Yuce, G. Aygun, L. Ozyuzer, Comparative study of annealing

and gold dopant effect on DC sputtered vanadium oxide films for bolometer applications, Opt. Quant. Electron (2017) 49:238.

[38] Bryan Douglas , The nano-composite nature of vanadium oxide thin films for use in infrared microbolometers A Dissertation in Materials Science and Engineering , Pennsylvania State University, USA (December 22, 2010).

[39] Wood, R.A. High-performance infrared thermal imaging with monolithic silicon focal planes operating at room temperature. in Electron Devices Meeting, (1993). IEDM '93. Technical Digest., International. 1993.

[40] Benhenni.I-Berrouane.W, Thermal anneling effect on thermal evaporated Vanadium oxides thin film, master diploma thesis in physics, option nanophysics of University of Saad Dahleb BLIDA 1 (2019).

[41] Wang, H., Yi, X., Chen, S.: Low temperature fabrication of vanadium oxide films for uncooled bolometric detectors. Infrared Phys. Technol. 47, 273–277 (2006).

[42] H. Alaboz,,Y. Demirhan, H. Yuce, G. Aygun, L. Ozyuzer, Comparative study of annealing and gold dopant effect on DC sputtered vanadium oxide films for bolometer applications, Opt Quant Electron (2017).

[43] Higashi, Paul (August 1966). (PDF).IEEE Transactions on Electronic Computers. EC-15 (4): 459–467. doi:10.1109/PGEC.1966.264353.

[44] O.belahssen, Elaboration and characterization of of thin-film gas sensor (El-Oued University) ,(November 2019).

[45] Matt Hughes,Article Published: (21 November 2014).

[46] M.Benkat Sunil Kumar Channam , Synthesis of strongly correlated oxides and investigation of their electrical and optical properties,thesis doctorate of the university of Toulouse , (Thursday, September 14, 2017).

[47] Hélary Doriane, Darque-Ceretti Evelyne, Bouquillon Anne, Aucouturier Marc, Monge

Gabriel. Contribution de la diffraction de rayons X sous incidence rasante à l'étude de céramiques lustrées. In: Revue d'Archéométrie, N°27, (2003). pp. 115-122.

[48] Jean M. Bennett, Lars Mattsson, Introduction to Surface Roughness and Scattering, Optical Society of America, Washington (1989), D.C.

[49] W J Walecki, F Szondy and M M Hilali, "Fast in-line surface topography metrology enabling stress calculation for solar cell manufacturing for throughput in excess of 2000 wafers per hour" (2008) Meas.

[50] Stout, K. J.; Blunt, Liam (2000). Three-Dimensional Surface Topography (2nd ed.). Penton Press.

[51] Binnig, Gerd, Calvin F Quate, and Ch Gerber (1986). "Atomic force microscope." Physical review letters 56.9 (1986): 930". Physical Review Letters.

[52] Chandra,H, Materials (2017).

[53] Manual for the Racal-Dana Databridge 9343M: "If the resistance value is low, less than 100 ohms, make a four-terminal connection...“, (3 October 1990).

[54] Behrendt, D. (September 1967). "Rod Memory Array Production Design". IEEE Transactions on Parts, Materials and Packaging. **3** (3): 77–81. doi:10.1109/TPMP.1967.1135727.

[55] Higashi, Paul (August 1966). "A Thin-Film Rod Memory for the NCR 315 RMC " (PDF). IEEE Transactions on Electronic Computers. EC-15 (4): 459–467. doi:10.1109/PGEC.1966.264353.

[56] JCPD Card [071-0565]

[57] C. Malerba, M. Valentini, C.L Azanza Ricardo, A. Rinaldi, E. Cappelletto, P. Scardi, A. Mittiga, Blistering in Cu_2ZnSnS_4 thin films: correlation with residual stresses, Materials & design 108, 725 (2016).

[58] Mechanics of functionnal thin films : instabilities and adhesion, Dissertation, Mechanics of materials, Université Pierre et Marie Curie, France (2013).

[59] H. E. EVANS, A. T. DONALDSON, and T. C. GILMOUR, Mechanisms of Breakaway Oxidation and Application to a Chromia-Forming Steel, Oxid. Met. 52, 379 (1999).

[60] Sang-Woon Hwang, Sami-ullah Rather, Mehraj-ud-din Naik, Chang Su Soo, Kee-Suk Nahm, Hydrogen uptake of multiwalled carbon nanotubes decorated with Pt–Pd alloy using thermal vapour deposition method, J. of Alloys and Compounds 480, 20 (2009).

[61] M. Nishikawa, T. Nakajima, T. Manabe, T. Okutani, T. Tsuchiya, High Temperature-Coefficient of Resistance at Room Temperature in W-Doped VO2 Thin Films on Al2O3 Substrate and Their Thickness Dependence, Materials Letters 64 (2010) 1921–1924.

[62] Bin Wang, Jianjun Lai, Hui Li, Haoming Hua, Sihai Chen; Nanostructured vanadium oxide thin film with high TCR at room temperature for microbolometer, Infrared Physics & Technology 57, 8 (2013) .

[63] M. Nishikawa, T. Nakajima, T. Manabe, T. Okutani, T. Tsuchiya, High Temperature-Coefficient of Resistance at Room Temperature in W-Doped VO2 Thin Films on Al2O3 Substrate and Their Thickness Dependence, Materials Letters 64 (2010) 1921–1924.

[64] Woods, D.F., Hough, C., Peel, D., Callaini, G., Bryant, P.J. (1996). Dlg protein is required for junction structure, cell polarity, and proliferation control in Drosophila epithelia. J. Cell Biol. 134(6): 1469--1482.

[65] Gauntt, Bryan Douglas, the nano-composite nature of vanadium oxide thin films for use in infrared microbolometers., thesis Pennsylvania State University, USA (December 22, 2010).